Insights on Global Warming

John H. Seinfeld
Dept. of Chemical Engineering, California Institute of Technology, Pasadena, CA 91125

DOI 10.1002/aic.12780
Published online October 11, 2011 in Wiley Online Library (wileyonlinelibrary.com).

The global temperature increase over the last century and a half (~ 0.8°C), and the last three decades in particular, is well outside of that which can be attributed to natural climate fluctuations. The increase of atmospheric CO_2 over this period has been conclusively demonstrated to be a result largely of fossil fuel burning. The global mean temperature change that results in response to a sustained perturbation of the Earth's energy balance after a time sufficiently long for both the atmosphere and oceans to come to thermal equilibrium is termed the Earth's climate sensitivity. The purely radiative (blackbody) warming from a doubling of CO_2 from its preindustrial level of 280 parts-per-million (ppm) to 560 ppm is ~ 1.2°C; the actual warming that would result is considerably larger owing to amplification by climate feedbacks, including that owing to water vapor. Increases in greenhouse gas (GHG) levels are estimated to have contributed about +3.0 W m^{-2} perturbation (radiative forcing) to the Earth's energy balance. Particles (aerosols), on the whole, exert a cooling effect on climate, with a total forcing estimated by the Intergovernmental Panel on Climate Change (2007)[1] as −1.2 W m^{-2}, a value that is subject to considerable uncertainty. If the actual magnitude of aerosol forcing is close to the low end of its estimated uncertainty range, then it offsets a considerably smaller fraction of the GHG forcing and the total net forcing is at the high end of its range, ~ 2.4 W m^{-2}; at the other extreme, if the actual aerosol cooling is at the high end of its range, then aerosol forcing is currently offsetting a major fraction of GHG forcing, and the total net forcing is only ~ 0.6 W m^{-2}. To explain the actual global increase in temperature of ~ 0.8°C, these two extremes have major implications in terms of the Earth's climate sensitivity. Climate sensitivity is determined by the strength of feedbacks, of which cloud feedback is the most uncertain. That the Earth has warmed and that GHGs are responsible is unequivocal; the Earth's climate sensitivity and the effect of aerosols complicate answers to the question: how much warming and how soon? © 2011 American Institute of Chemical Engineers *AIChE J,* 57: 3259–3284, 2011
Keywords: global warming, climate sensitivity, greenhouse gases

Introduction

Earth's climate is the result of a balance between incident solar (shortwave) radiation absorbed and thermal infrared (longwave) radiation emitted. Averaged over the globe and over a sufficiently long period of time, this balance must be zero. Because virtually all the energy for the climate system comes from the Sun, globally the amount of incoming solar radiation on average must be equal to the sum of the outgoing reflected solar radiation and the outgoing infrared longwave radiation emitted by the climate system. A perturbation of this global radiation balance, be it anthropogenic or natural, is called radiative forcing.

Correspondence concerning this article should be addressed to J. H. Seinfeld at seinfeld@caltech.edu.

Earth's surface temperature has increased by about 0.8°C over the past century.[1] The temperature increase has been particularly pronounced in the past 30 years. The global temperature increase over the last century and a half, and the last three decades in particular, is well outside of that which could be attributed to natural climate fluctuations; only a substantial positive climate forcing (a perturbation to the Earth's energy balance that results in more absorption of solar incoming radiation than emission of infrared outgoing radiation) could produce such an increase. Solar insolation has remained essentially constant over the past 5 to 6 decades and therefore cannot explain the degree of warming that has occurred over that time, and the changes in solar output over the Sun's 11-year sunspot cycles do not exert a net long-term influence on climate. From a comprehensive analysis of all evidence, the inescapable conclusion is that no natural climate factor can be the cause of this temperature increase.

Atmospheric carbon dioxide concentrations are higher today than at any time in at least the past 650,000 years. They are about 35% higher than before the Industrial Revolution. Carbon dioxide is an absorber of terrestrial infrared radiation, a so-called greenhouse gas (GHG), as are methane (CH_4), nitrous oxide (N_2O), water vapor, and a number of other trace gases. The atmospheric concentrations of CO_2 and other greenhouse gases have been measured continuously since the late 1950s. Since then, CO_2 concentrations have increased steadily from about 315 parts per million (ppm, or molecules of carbon dioxide per million molecules of dry air) in the late 1950s to about 390 ppm now. The amount of CO_2 in the air is currently increasing about 2 ppm per year. Continuing on a business-as-usual path of fossil-fuel energy use, and accounting for projected population growth, the CO_2 level will be $\sim$ 900 to 1100 ppm by the end of this century. Atmospheric concentrations of greenhouse gases can be measured in bubbles of ancient air preserved in ice (e.g., in Greenland and Antarctica). Ice core records currently go back 650,000 years. Before the Industrial Revolution, levels were about 280 ppm, and have varied naturally about 180 ppm during ice ages and 300 ppm during warm periods. Concentrations of methane and nitrous oxide have likewise increased since the Industrial Revolution and, for methane, are higher now than they have been in the past 650,000 years.

With respect to global warming, as concisely stated by Keller,[2] the primary issues are—how much and how soon? The goal of the present review is to present the essential elements of climate change in a manner that the current state of scientific understanding and especially the confidence with which one may predict future climate is appreciated. We follow a logical sequence in the presentation, beginning with the Earth's energy balance, proceeding to the concepts of radiative perturbation (or forcing), climate sensitivity (the change in global mean temperature in response to a given perturbation of the Earth's energy balance), and climate feedbacks (amplifications of warming owing to internal responses to warming within the climate system). We then discuss climate forcing agents, including the Sun itself, cosmic rays, and those substances that exert a radiative perturbation on the Earth's energy balance. These include the well-mixed greenhouse gases, ozone, and aerosols (airborne particles). In an analysis of estimated contributions to the total climate forcing, it is seen that the radiative perturbations due to aerosols represents the most important uncertainty in determining the Earth's climate sensitivity. After discussing each of these components of the climate system, we use a single-compartment model of the atmosphere-land-ocean system to derive the Earth's blackbody climate sensitivity. With a simple feedback analysis, we derive expressions for the feedback factors that describe the amplification and dampening of a radiative perturbation by different components of the climate system, and we discuss water vapor, lapse rate (the atmospheric temperature profile), and cloud feedbacks. The remainder of the article addresses climate issues that are sometimes cited as not sufficiently well understood to accept the overwhelming weight of science concerning the causes of the current warming; these include the paleoclimate record, glacial-interglacial cycles, temperature reconstructions, ice sheets and sea ice, and sea level rise.

The Earth's Energy Balance

Annually averaged, the Earth receives 341 W m^{-2} of solar radiation at the top of the atmosphere[3] (Figure 1). Of this amount, $\sim$ 102 W m^{-2} is reflected back to space by the surface of the Earth and by clouds and particles (aerosols) in the atmosphere. As a result, the net radiant energy absorbed by the Earth is 239 W m^{-2}. At thermal equilibrium, 239 W m^{-2} of energy must be radiated back to space from the Earth, establishing the equilibrium temperature of the Earth. The equilibrium climate is, more precisely, a quasi-equilibrium climate, owing to the fact that changes do occur on millennial and longer timescales, such as glacial-interglacial cycles caused by orbital variations. Global average surface temperature is about 288 K (15°C), for which the corresponding blackbody irradiance is 396 W m^{-2}. Much of this infrared energy emitted at the Earth's surface is absorbed by molecules in the atmosphere, such as carbon dioxide (CO_2), water vapor, methane (CH_4), nitrous oxide (N_2O), chlorofluorocarbons, and ozone (O_3) and re-emitted in both upward and downward directions, further heating the Earth's surface and maintaining the atmospheric temperature gradient. At equilibrium, the emitted longwave flux at the top of the atmosphere, 239 W m^{-2}, is considerably less than that emitted at the surface, 396 W m^{-2}. The reader is referred to the comprehensive analysis of the Earth's energy budget of Trenberth et al.[3] As compared with the average annual energy input to the Earth from the Sun, the amount of energy released annually as a result of humanity's energy production[4] is about 0.025 W m^{-2}. Internal terrestrial energy generation[5] is $\sim$ 0.087 W m^{-2}. Human energy production, therefore, is totally negligible as compared with energy flows associated with solar and terrestrial radiation.

Earth's surface is heated by absorption of solar radiation; it emits infrared radiation, which would escape almost directly to space if it were not for the presence of water vapor and the other greenhouse gases. Nitrogen and oxygen, which account for about 99% of the volume of the atmosphere, are essentially transparent to infrared radiation. Greenhouse gases absorb infrared radiation and re-emit it in all directions. Some of the infrared radiation that would

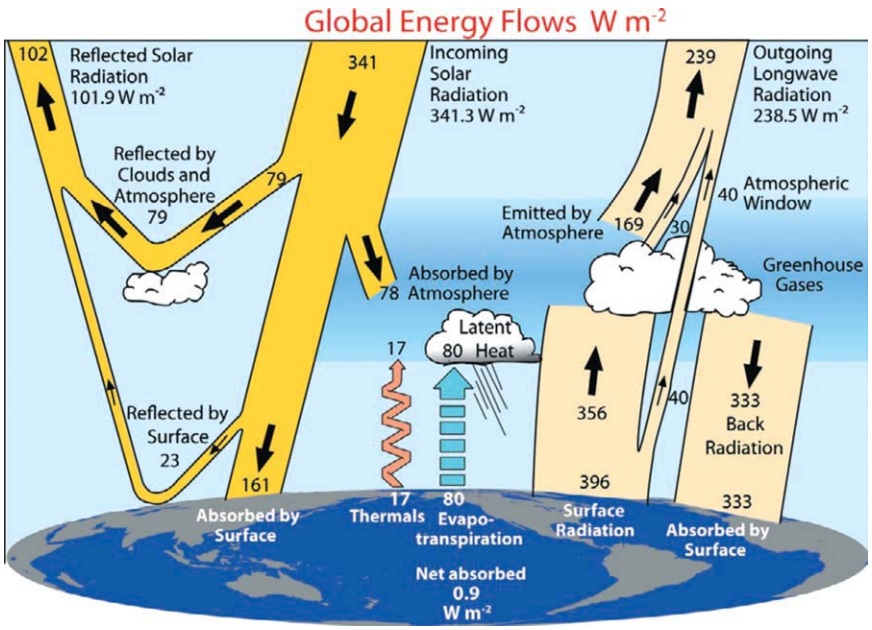

Figure 1. Earth's energy balance.[3] Incoming and outgoing energy fluxes from Earth on an annual-average basis.

The greenhouse effect refers to the absorption and reradiation of energy by atmospheric gases, resulting in a downward flux of infrared radiation from the atmosphere to the surface. At equilibrium, the total rate at which energy leaves the Earth (102 W m^{-2} of reflected sunlight plus 239 W m^{-2} of infrared radiation) is equal to 341 W m^{-2} of incident sunlight. [Color figure can be viewed in the online issue, which is available at wileyonlinelibrary.com.]

otherwise directly escape to space is emitted back toward the surface. Without this natural greenhouse effect, primarily owing to water vapor and carbon dioxide, Earth's mean surface temperature would be a freezing −18°C, instead of the habitable 15°C. Despite their small amounts, the greenhouse gases profoundly affect Earth's temperature.

Emission of thermal longwave radiation in the troposphere depends on the temperature of the atmosphere at the altitude at which it is emitted. In the troposphere, the temperature generally decreases with height. Effectively, infrared longwave radiation emitted to space originates from an altitude with a temperature of, on average, −19°C, in balance with the net incoming solar radiation, whereas the Earth's surface is at a temperature of, on average, +15°C. An increase in the concentration of greenhouse gases leads to an effective radiation into space from a higher altitude at a lower temperature.

The troposphere is characterized by constant vertical motion; in the process of rising, the air cools by expansion, and the temperature decreases with height. Solar energy is primarily absorbed at the Earth's surface and transferred to the atmosphere by surface heat fluxes. Convection and other heat transport mechanisms connect all levels in the troposphere, and, to a good approximation, the troposphere can be considered to warm and cool as a unit. When a greenhouse gas is present, the upwelling infrared radiation from the surface is absorbed and re-emitted. As a result, the infrared radiation that actually escapes to space comes from the higher, colder parts of the atmosphere. As the emission rate of radiation from a black body varies with the fourth power of temperature, the flux of radiation from these upper levels is considerably less than that which is emitted from the surface. By contrast, the downwelling radiation to the surface comes predominantly from the warmer layers nearest the surface. Earth's clouds, whether liquid or frozen water, act essentially as black bodies. They emit at the cloud-top temperature, which is cold if the cloud tops are in the mid-to upper troposphere.

Infrared radiation emitted by the Earth has a maximum near 10 μm wavelength. Oxygen and ozone absorb radiation strongly in the ultraviolet region, but their absorption is essentially zero in the visible and infrared regions. Methane absorbs strongly in two narrow regions around 3.5 and 8 μm wavelength, which are in the infrared portion of the spectrum. Nitrous oxide has absorption peaks at about 5 and 8 μm. The CO_2 molecule has four main groups of absorption features in the thermal infrared, of which the most important is that at wavelength near 15 μm. As a polar molecule, water vapor has a richer set of vibrational and rotational modes that allows it to absorb infrared photons over a much broader range of wavelengths than CO_2. Water vapor is so abundant in the atmosphere that in those regions of the spectrum where H_2O vapor absorbs infrared radiation, the spectrum is saturated. CO_2 and CH_4 have absorption in some of the "windows" in the infrared spectrum where H_2O vapor does not absorb and where terrestrial radiation escapes. The radiative forcing change owing to an incremental change in CO_2 abundance is not linear but is approximately proportional to the logarithm of the CO_2 mixing ratio. For a relatively small change in CO_2 abundance, considering that $\ln(1+\varepsilon) \cong \varepsilon$, the forcing change due to a change in CO_2 can be calculated as linearly proportional to the change in CO_2. The

CO_2 greenhouse effect is directly visible in satellite observations as the bite taken out of the infrared spectrum near 15 μm wavelength, a feature the details of which agree precisely with first-principles radiative transfer calculations.[6]

Radiative Forcing

Radiative forcing, measured in units of watts per square meter (W m^{-2}), is any imposed perturbation on the Earth's energy balance.[7] It is the imbalance, or disequilibrium, caused by the forcing agent between the solar energy absorbed by the Earth and thermal emission by the Earth back to space. Therefore, radiative forcing is the amount by which the forcing mechanism would change the top-of-the-atmosphere energy budget, if the temperature were not allowed to change so as to restore equilibrium. Radiative forcing is customarily computed with all tropospheric properties held fixed at their unperturbed values, and after allowing for stratospheric temperatures, if perturbed, to readjust to radiative-dynamical equilibrium. Radiative forcing is called instantaneous if no change in stratospheric temperature is accounted for. A forcing is taken as positive if it tends to make the Earth warmer, that is, if the solar input exceeds the thermal (infrared) output. An example of positive forcing is an increase in the luminosity of the Sun. A large volcanic eruption that injects particles into the lower stratosphere, which reflect more sunlight back to space than in nonvolcanic periods, is exemplary of a negative forcing, which is expressed as negative in sign.

Climate sensitivity

The change in climate that results from an imbalance in the Earth's energy balance is manifested in a number of ways: temperature, precipitation, snow and ice cover, etc. The index that is used most commonly as a measure of climate change is the annual and global-mean surface air temperature. In assessing the extent to which climate has changed, one usually defines a temperature anomaly, the difference in temperature at a given site relative to a climatological mean temperature at that site.

The global mean temperature change that results in response to an imposed and sustained perturbation on the Earth's energy balance after a time sufficiently long for both the atmosphere and the oceans to come to thermal equilibrium is termed the Earth's climate sensitivity. Climate sensitivity has units of temperature change per W m^{-2} (°C W^{-1} m^2 or K W^{-1} m^2) and is given the symbol λ. Two assumptions inherent in this definition of climate sensitivity are that a change in global-mean surface temperature is directly proportional to the imposed forcing and that different forcings are additive in contributing to a total forcing. Both of these assumptions are supported by climate models. There are two approaches to determining climate sensitivity. The empirical approach is based on an observed change in global mean temperature over a given historical time period with respect to an estimated or known forcing. The second way of determining climate sensitivity is based on simulations using climate models.

A standard benchmark that is used to assess climate change is a doubling of CO_2 from its preindustrial level of about 280 ppm to 560 ppm. (This scenario is referred to in shorthand notation as $2xCO_2$.) The perturbation to the Earth's energy balance that would result from $2xCO_2$ is $\sim$ 3.7 W m^{-2}. The increase in the global mean temperature required to re-equilibrate the Earth's energy balance to this change, considering solely the Earth's blackbody Stefan-Boltzmann response, is 1.2°C. A temperature increase of 1.2°C in response to a forcing of 3.7 W m^{-2} implies a climate sensitivity of 0.32°C W^{-1} m^2. The IPCC[1] estimate of the equilibrium global-mean temperature change that would result from $2xCO_2$ is 3°C, uncertain to a factor of 2 between the low and high ends of the uncertainty range (66% likelihood that the actual sensitivity lies within the uncertainty range). The corresponding climate sensitivity is 3°C/3.7 W m^2 = 0.81°C W^{-1} m^2. The estimated global mean temperature increase of 3.0°C from a doubling of CO_2 represents, therefore, an amplification by a factor of about 2.5 over the purely blackbody temperature change of 1.2°C.

Climate feedbacks

The explanation of why the actual temperature change is so much larger than that based purely on the amount of absorbed radiation lies in climate feedbacks. Once the Earth starts to warm, in response, say, to an increase in greenhouse gas levels, other changes take place that act to amplify the initial warming. A warmer atmosphere holds more water vapor, which itself is a powerful infrared absorber. Also, as temperature increases, sea ice begins to melt. Because the darker ocean absorbs more sunlight than the sea ice it replaced, this leads to further warming. These feedbacks are positive, in that they act to amplify (rather than retard) the effect of the initial perturbation.

The well-mixed greenhouse gases (CO_2, CH_4, N_2O, chlorofluorocarbons) do not condense or precipitate from the atmosphere, whereas water vapor and clouds respond rapidly to local meteorology by evaporating, condensing, and precipitating. As a result, changes of water vapor and clouds constitute fast feedback processes in the climate system. Of the overall greenhouse effect on Earth, including the effect of climate feedbacks, water vapor accounts for $\sim$ 50%, clouds $\sim$ 25%, CO_2 itself $\sim$ 20%, and the minor GHGs $\sim$ 5%. At present, CO_2 accounts for about one-third of the clear-sky greenhouse effect in the tropics and a greater portion in the drier, colder extratropics. Most of the remainder is due to water vapor. Despite its only fractional contribution to the greenhouse effect, CO_2 is, in fact, the controller of climate. If CO_2 were removed from the atmosphere, the atmosphere would cool sufficiently that much of the water vapor would precipitate out. That loss of water vapor would lead to further cooling, with still more water vapor removal, ultimately spiraling the planet into a globally glaciated state. It is the presence of CO_2 that maintains a level of warmth to keep the atmospheric level of water vapor that sustains our climate. Of course, increasing CO_2, and warming the atmosphere produces the opposite effect, additional warming, through positive water vapor feedback. In summary, the 25% contribution due to the noncondensing, long-lived GHGs supports and sustains the entire greenhouse effect, with the remaining 75% a result of the fast feedbacks involving water vapor and clouds.[8] Subsequently, we will discuss climate

feedbacks in more detail, but it is important to stress that the presence of the well-mixed GHGs in the atmosphere (especially CO_2) provides the basis for our present climate, upon which the fast feedback processes operate.

Time scales of climate change

If the Earth's radiation balance is perturbed, the global surface temperature will adjust so as to re-establish a balance between incoming and outgoing radiation. The Earth's radiation balance can be perturbed in a number of ways, for example: (1) A change in solar output of energy (either positive or negative) alters the solar radiation flux S_o; (2) A large volcano injects particles directly into the stratosphere – these particles reflect a portion of incoming solar radiation back to space and thereby prevent that radiation from reaching the Earth's surface, increasing the Earth's albedo A; (3) An increase in the concentration of infrared absorbing gases in the atmosphere leads to increased absorption of the Earth's longwave radiation, which reduces the outgoing infrared energy flux at the top of the atmosphere—in this case, the incoming solar energy flux then exceeds the outgoing energy flux, and the Earth has to warm as a consequence.

The climate response time is that needed for the climate system or its components to re-equilibrate to a new state, following a forcing resulting from external and internal processes or feedbacks. The response time of the troposphere is relatively short, from days to weeks, whereas the stratosphere reaches equilibrium on a time scale of typically a few months. Most of the heat capacity of the Earth is provided by the ocean. The upper 100 m or so of the ocean is efficiently mixed by wind stress and convection. The thermal inertia of this ocean mixed layer, by itself, would produce a surface temperature response time of about a decade. Experiments with climate models show that, in response to an instantaneous doubling of CO_2, about 40% of the equilibrium response is attained in $\sim$ 5 years, followed by a slow warming on century time scales, owing to exchange between the mixed layer and the deeper ocean. Climate feedbacks, which drive the ultimate temperature change, operate on an initial temperature change, not on the forcing. Thus, the climate response time depends on the climate sensitivity itself, as well as on the rate at which heat is transported into the deeper ocean. The rate of ocean heat uptake determines the planetary energy imbalance, which is the portion of the net climate forcing to which the planet has not yet responded. The Earth's energy imbalance is currently 0.6–0.7 W m^{-2}. This imbalance is a fundamental characterization of the state of the climate. It determines the amount of additional temperature change "in the pipeline." In the terminology of climate change, the transient temperature lags behind the equilibrium temperature.

Under equilibrium climate conditions, the solar heat flux to the upper layer of the ocean is balanced by a heat flux from the ocean to the atmosphere, and that balance establishes the temperature of the ocean surface layer. Heat transfer between the ocean and atmosphere is controlled by a thin layer at the ocean surface through which heat is transferred by conduction. The temperature gradient across this thin conduction layer determines the heat flux. If the GHG concentration in the atmosphere were to suddenly increase, the increased absorption of infrared radiation by GHGs leads to a downward heat flux that slightly increases the surface temperature, decreasing the flux of heat through the layer to the atmosphere. And, more of the energy acquired by the bulk of the ocean surface layer from absorption of solar radiation remains in the ocean, leading to an increased temperature of the upper layer of the ocean. Short-term absorption of heat is concentrated in the upper 100 m or so of the ocean. The time scale for transport from the surface layer into the deeper ocean is of order decades to centuries.

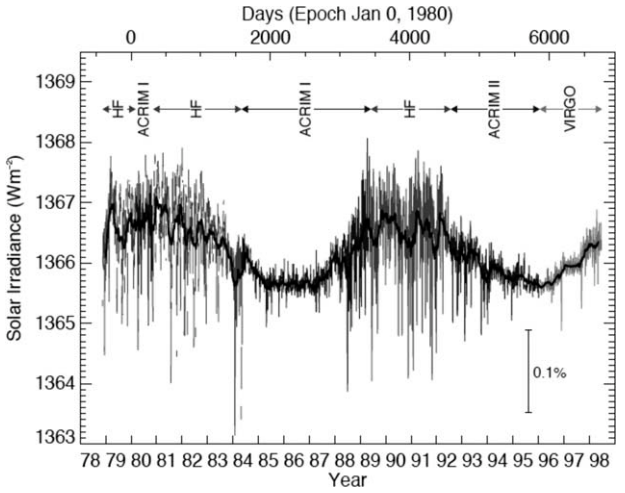

Figure 2. Total solar irradiance observations since 1978.

Since November 1978, a set of total solar irradiance (TSI) measurements from space is available. From measurements made by several different instruments a composite record of TSI can be constructed. Description of the procedures used to construct composites can be found in Fröhlich.[9]

Climate Forcing Agents

Solar irradiance

Total solar irradiance (TSI) is the amount of solar radiance received outside the Earth's atmosphere on a surface normal to the incident radiation and at the Earth's mean distance from the Sun. The most reliable measurements of solar radiation are made from space, and the precise satellite record extends back only to 1978. The generally accepted value of TSI is 1368 W m^{-2}, with an accuracy of about 0.2%. Variations of a few tenths of a percent are common, usually associated with the passage of sunspots across the solar disk. The solar cycle variation of TSI is of the order of 0.1%.

Since 1978, solar irradiance has been measured with high precision from satellites (Figure 2); before that, sunspot observations provide a measure of solar activity. In addition, cosmogenic radionuclides, ^{10}Be and ^{14}C, serve as proxies to extend solar activity reconstructions beyond the period of direct observations. Produced in the atmosphere by galactic cosmic rays, these radionuclides have decreased production

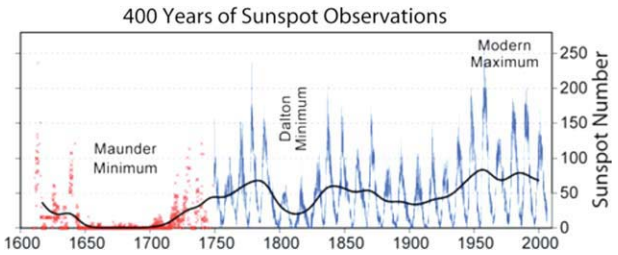

Figure 3. Record of sunspot observations over the period 1600—present day.

Two periods of especially cool temperatures, the Maunder Minimum (also referred to as the Little Ice Age) ~ 1650 to 1750, and Dalton Minimum ~ 1800 to −1850, correspond to low sunspot number. [Color figure can be viewed in the online issue, which is available at wileyonlinelibrary.com.]

rates during periods of high solar activity. Their records exist in ice cores (^{10}Be) and tree rings (^{14}C).[10]

Understanding the relationship between solar variability and the Earth's climate is of prime importance when assessing the anthropogenic role in climate change.[11] Solar irradiance varies slightly over an 11-year cycle due to variation in the Sun's magnetic activity. Sunspots, dark regions on the solar disk, have been used to track fluctuations in the strength of the Sun's 11-year activity cycle for almost 400 years (Figure 3). Variations in satellite records of lower troposphere temperatures since 1978, in upper ocean temperatures since 1955, and in surface temperatures during the past century are approximately in phase with this 11-year solar cycle.[12] More sunspots equate to higher solar output. The so-called Maunder Minimum, or Little Ice Age, which lasted from 1650 to about 1800, was characterized by very low sunspot activity and unusually cold temperatures over Europe.

Direct radiative forcing owing to increases in total solar irradiance since 1750 is estimated by IPCC[1] to be +0.12 (−0.06, +0.18) W m^{-2}. Amplification of changes in total solar irradiance by the climate system itself has led to a ~ 20 year lag in the climate response.[13] For example, climate models predict that the lower Northern Hemisphere temperatures in the period 1650–1850 are a result of decreased solar activity that forced a shift of the North Atlantic Oscillation (NAO)/Arctic Oscillation (AO) with a lag of 20 years.[14] Eichler et al.[13] analyzed a 750-year ice core oxygen isotope record from the continental Siberian Altari (Figure 4). The strong correlation between reconstructed temperature and solar activity suggests solar forcing as the main driver for temperature variations over the period 1250–1850 in this region. From 1850 on, solar forcing became less important and only CO_2 concentration shows a significant correlation with the temperature record.

The period of greatest warming over the past century or so has occurred since 1970, and if the Sun is responsible for this warming, a sustained increase in solar irradiance would have to be evident in the satellite record. That record (Figure 2) indicates no net increase in solar irradiance since 1978, and reconstructions of pre-satellite data show this period of quiescence extends back to 1940. In a statistical analysis of solar output and Earth's temperature variations, Krikova and Solanki[15] assumed that the Sun was totally responsible for the change in Earth's temperature before 1970 and that this interplay persisted after 1970. Then, using reconstructions and measured records of solar output, they estimated the fraction of the dramatic temperature rise after 1970 that could be due to the influence of the Sun. The analysis shows definitively that since 1970 the solar influence on climate could not be a significant cause of the observed temperature increase.

The average global variation of surface temperature over the 11-year solar cycle is ~ 0.2°C, corresponding to a change in radiative forcing from solar-min to solar-max of ~ 0.18 W m^{-2}.[16] This amount of temperature change is too large to be explainable purely by the direct effect of a 0.18 W m^{-2} variation in total solar intensity. The actual observed temperature response is the result of the positive feedbacks inherent in the climate system. The inferred climate sensitivity based on the climate response to sunspot cycles is thus

$$\lambda = \frac{0.2^{o}\mathrm{C}}{0.18\ \mathrm{W\ m^{-2}}} \sim 1\,\frac{^{o}\mathrm{C}}{\mathrm{W\ m^{-2}}}$$

As this climate sensitivity is a transient, rather than an equilibrium sensitivity (i.e., the climate has not come to equilibrium in response to the varying solar output), and as the equilibrium climate sensitivity always exceeds the transient sensitivity, this method of inferring climate sensitivity leads to a value exceeding 1°C W^{-1} m^2, implying a climate sensitivity that is near the upper end of that predicted by climate models.

Haigh et al.[17] have shown based on daily measurements of the solar spectrum between 0.2 and 24 μm wavelength, made by the Spectral Irradiance Monitor (SIM) on the Solar Radiation and Climate Experiment (SORCE) satellite, since 2004 that over this declining phase of the solar cycle that peaked in 2000–2002 there was a 4–6 times larger decline in ultraviolet radiation than would have been predicted based

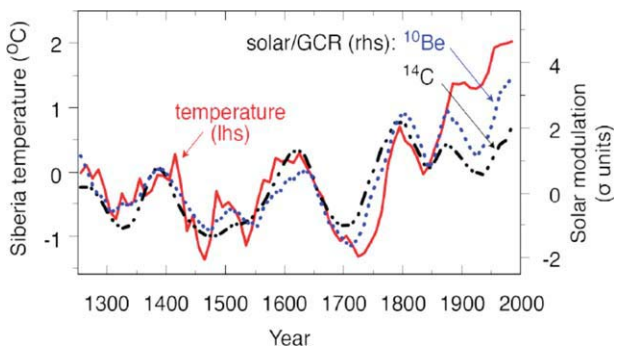

Figure 4. Temperature in Siberia from glacial ice core data and galatic cosmic ray fluxes derived from ^{10}Be and ^{14}C.

Before about 1850, a distinct correlation exists between cosmic ray flux and temperature in Siberia, although no physical link has been established. After about 1850, the correlation ceases to exist. [Color figure can be viewed in the online issue, which is available at wileyonlinelibrary.com.]

on previous understanding. This reduction was partially compensated in total solar output by an increase in radiation at visible wavelengths. While these new data do not alter the overall understanding of the role of solar output changes in governing climate, they do suggest that the detailed spectral distribution of solar output over solar cycles may not be fully understood.

The deepest, most prolonged solar minimum in the period of accurate solar monitoring since the late 1970s has occurred in the 2005–2010 period. An estimate of the Earth's energy imbalance during this period provides a test of the effect of solar variability on climate, as the imbalance is the net effect of the reduced solar irradiance and all other radiative forcings. The best current estimate of the net planetary energy imbalance over the 2005–2010, solar minimum based on ocean measurements, is $+0.5$ W m^{-2}. That this estimate is strongly positive is a fundamental verification that human-induced climate forcing, not solar variability, is the dominant driving force for climate change.

Carbon dioxide

That the increase in the atmospheric level of CO_2 over the past century or so is a result largely of fossil-fuel burning is conclusively demonstrated from several lines of evidence. These include: (1) records of coal, oil, and natural gas consumption; and (2) concomitant decreases in the relative abundance of both the stable (^{13}C) and radioactive (^{14}C) carbon isotopes and the decrease in atmospheric oxygen. Adding up the human sources of CO_2 primarily from fossil fuel burning, cement production, and land use changes (e.g., deforestation), one finds that about 56% of the CO_2 emitted as a result of human activities is accumulating in the atmosphere. The other 44% of the emitted carbon dioxide is being taken up by oceans and the biosphere. The CO_2 sinks may begin to saturate eventually, but so far there is no evidence of this. Emissions of CO_2 from human activities can account for the increase in atmospheric CO_2 concentrations. Changes in the isotopic composition of CO_2 show that the carbon in added CO_2 derives largely from plant materials, that is, from processes such as burning of biomass or fossil fuels, which are derived from fossil plant materials. Minute changes in the atmospheric concentration of oxygen show that the added CO_2 derives from burning of the plant materials. Concentrations of CO_2 in the ocean have increased along with the atmospheric concentrations, showing that the increase in atmospheric CO_2 cannot be a result of release from the oceans. All lines of evidence taken together lead to the unambiguous conclusion that the increase in atmospheric CO_2 concentrations is primarily a result of fossil fuel burning. Similar reasoning can be invoked for other greenhouse gases, but for some of those, such as methane and nitrous oxide, their sources are not as clear as those of CO_2.

Carbon in CO_2 has two naturally occurring stable isotopes, ^{12}C and ^{13}C. ^{12}C constitutes about 99% of the C in CO_2, with ^{13}C being about 1%. The $^{13}C/^{12}C$ ratio in CO_2 emitted from fossil fuel combustion is less than that in atmospheric CO_2, so that when CO_2 from fossil fuel combustion enters the atmosphere, the $^{13}C/^{12}C$ ratio in atmospheric CO_2 decreases at a rate that can be predicted based on the magnitude of fossil fuel emissions. (The $^{13}C/^{12}C$ ratio in CO_2 can be measured at 1 part in 10^5). The energetics of photosynthesis lead to a preference for $^{12}CO_2$ over $^{13}CO_2$, as slightly less energy is required to bond to $^{12}CO_2$ than $^{13}CO_2$. Thus, the naturally occurring $^{13}C/^{12}C$ ratio is skewed toward ^{12}C in plants. Fossil fuels were originally plants, so fossil fuel CO_2 is depleted in ^{13}C. ^{13}C fractions have also decreased in ocean surface waters over the past decades. Such behavior is consistent with an atmospheric fossil fuel source of CO_2 and inconsistent with an oceanic source. Oceanic carbon has slightly more ^{13}C than atmospheric carbon, but $^{13}CO_2$ is heavier and less volatile than $^{12}CO_2$; as a result, CO_2 degassed from the ocean has a ^{13}C fraction close to that of atmospheric CO_2. It is not possible therefore, that an oceanic source of CO_2 could lead to a simultaneous drop of ^{13}C in both the atmosphere and the ocean. Finally, if heating of the oceans were the source of atmospheric CO_2, a trend of decreasing concentration of CO_2 would be expected; yet, what is observed is the opposite – CO_2 concentrations in the ocean have risen even as ocean temperature has risen.[18] The unstable carbon isotope ^{14}C termed radiocarbon, comprising about 1 in 10^{12} carbon atoms in the atmosphere, has a half-life of 5700 years. The stock of ^{14}C is replenished in the upper atmosphere by the interaction of cosmic rays with ^{14}N. Fossil fuels contain no ^{14}C, so emission of CO_2 from burning fossil fuels lowers the atmospheric ^{14}C fraction. Atmospheric ^{14}C, measured in the tree rings, decreased by 2 to 2.5% from about 1850 to 1954, when atmospheric nuclear testing began to inject ^{14}C into the atmosphere. The observed decline in ^{14}C cannot be explained by a CO_2 source from terrestrial vegetation or soils.

Volcanic emissions of CO_2 arise from erupting magma and from degassing of unerupted magma beneath volcanoes. Over very long time scales, these CO_2 emissions act to restore CO_2 lost from the atmosphere and oceans by silicate weathering, carbonate deposition, and organic carbon burial. Global estimates of the annual present-day CO_2 volcanic emissions range from 0.15 to 0.26 gigaton per year; this is to be compared with anthropogenic CO_2 emissions, estimated at 35 gigatons in 2010.[19] (The level of global volcanic CO_2 emissions is roughly comparable in magnitude to that emitted annually by the state of Florida.) Moreover, if atmospheric CO_2 increases over the past century were the result of volcanic missions, not anthropogenic activity, the massive eruption of Mt. Pinatubo in 1991 would have been accompanied by a large pulse in CO_2. No CO_2 pulse appeared in any global measurements, and, in fact, the main effect of the eruption was a temporary cooling from the increased reflection of sunlight by the resulting stratospheric aerosols.

Methane

The global methane concentration has increased by a factor of 2.5 since 1800, with an associated radiative forcing of about 0.5 W m^{-2}. Methane is oxidized in the atmosphere by hydroxyl radicals to CO, and eventually to CO_2, with an atmospheric lifetime of about 10 years. Increases in CH_4 lead to an increase in stratospheric water vapor (about 7% of CH_4 is oxidized in the upper atmosphere) and to an increase in tropospheric O_3 through reactions involving oxides of nitrogen, thus having an indirect effect on forcing through stratospheric water vapor and ozone production. If these

additional indirect effects are accounted for, the full contribution of CH_4 to radiative forcing[21] is closer to 0.9 W m^{-2}.

Ozone

Estimating the radiative forcing attributable to the increase in tropospheric ozone since preindustrial times is hampered by a lack of knowledge of the global ozone level at that time. That uncertainty stems not from a poor understanding of the atmospheric processes generating ozone but rather from lack of knowledge of 19th Century precursor emissions. Ozone is not directly emitted; it is produced by chemistry involving oxides of nitrogen (NO_x), CH_4, CO, and nonmethane volatile organic compounds. Surface ozone concentrations at the end of the 19th Century have been estimated as about 10 ppb, but this estimate is based on limited data. Current global chemical transport models, upon removal of anthropogenic NO_x, CO, CH_4, and nonmethane volatile organic compound emissions, predict the order of 20 ppb of O_3.[21] Despite the uncertainty in the preindustrial level of ozone, the current estimate of ozone radiative forcing owing to the difference in tropospheric ozone abundance between preindustrial and present day is comparable to that of methane. Anthropogenic radiative forcing from tropospheric ozone is estimated in the range of 0.25 to 0.65 W m^{-2}, with a median value of 0.35 W m^{-2}. Roughly two-thirds of the current O_3 radiative forcing is attributed to the increase in CH_4 over this period.

Magnitude of climate forcing of greenhouse gases

The magnitude of climate forcing for a greenhouse gas can be expressed as W m^{-2} of forcing per unit of increase of atmospheric concentration. The relative strengths of CO_2, CH_4, and N_2O at their present levels, expressed as W m^{-2} per ppm, are:

CO_2(380 ppm)	0.0044	W m^{-2} ppm^{-1}
CH_4(1.8 ppm)	0.2706	
N_2O(320 ppb)	0.5106	

Per unit part-per-million increase, CH_4 and N_2O are 62 and 114 times as effective in radiative forcing as CO_2; however, CH_4 is 200 times less abundant than CO_2, and N_2O is $\sim$ 1000 times less abundant, so CO_2 exerts the dominant effect.

Aerosols

Particles in the atmosphere, referred to as aerosols, arise from natural sources such as wind-borne dust, sea-spray, natural fires and emission of biogenic volatile organic carbon. They also arise from a range of anthropogenic activities, such as the combustion of fossil fuels and biofuels. Emitted directly as particles (primary aerosol) or formed in the atmosphere by (often photochemical) conversion of gaseous precursors (secondary aerosol), atmospheric particles range in size from a few nanometers to tens of micrometers.

Tropospheric aerosols play an important role in the global climate system through modifications of the global radiation budget. Aerosols scatter and absorb solar radiation and serve as the seed particles on which cloud droplets form. Through scattering and absorption of solar radiation, aerosols reduce solar insolation at the surface, leading to changes in surface fluxes of energy and water, with concomitant changes to the hydrological cycle. Aerosols containing absorbing material, such as black carbon, also heat the atmosphere, altering profiles of temperature and relative humidity and consequently atmospheric stability. Aerosols have a tropospheric lifetime measured in weeks; because of this, aerosol levels are highly nonuniform over the Earth, with highest concentrations occurring in regions of highest emissions. Aerosols injected into the stratosphere, such as from a volcanic eruption, have a lifetime of a year or more, owing to the absence of removal mechanisms (wet and dry deposition) present in the troposphere. Because aerosols interact with solar radiation, their forcing occurs only during daylight hours.

Changes in aerosol levels can change cloud properties through alteration of the number of activated droplets; changes in cloud properties can then lead to changes in cloud reflectivity, cloud lifetime, and precipitation. Numerous observations, at the local scale, show that an increase of ambient aerosol concentrations enhances the reflective properties of low (warm) clouds as well as their lifetimes. Globally, these effects lead to a negative radiative forcing or global cooling. The uncertainty in the magnitude of this cooling will likely be reduced somewhat as model studies are reconciled with in situ aircraft observations and satellite data; globally the radiative forcing from this effect is likely in the range of -1 to -1.5 W m^{-2}. Any regional or global changes in cloud properties will have immediate consequences to the Earth's energy balance. On the whole, the estimated change in aerosol levels from preindustrial time is calculated to have exerted a cooling effect on climate.

The amount and properties of Cloud Condensation Nuclei (CCN) determine the initially formed cloud droplets, but environmental conditions such as temperature and humidity profiles, winds, and surface fluxes of heat and moisture determine whether a cloud grows or wanes. Changes in aerosol concentrations produce changes in the size distribution of cloud droplets. An increase in CCN leads to more numerous and smaller droplets. Droplet growth by collision-coalescence becomes less efficient, delaying the formation of large droplets and causing a delay or suppression of downdrafts and warm rain. The resulting updrafts may be stronger due to the latent heat of water condensation in the absence of a balance by downdrafts due to large drops. Stronger updrafts lift the smaller droplets upward, increasing cloud top height. The smaller droplets lifted upward will freeze at higher altitudes, releasing latent heat and further increasing convection. The presence of absorbing aerosols can change the atmospheric thermal profile by heating the aerosol layer while cooling the layers below. This process may stabilize shallow layers, reduce their relative humidity, suppress surface fluxes and shallow cloud formation inside or below the aerosol layer.[22,23]

Low clouds account for about half of the solar energy that is reflected back to space. Exactly how much additional cloud cooling would result from increased aerosol levels is a subject of intense study by the scientific community. The response of clouds to changing aerosol concentrations depends on local temperature and humidity, atmospheric dynamics, as well as the properties of the clouds themselves. Warm clouds, those made up of liquid drops, grow deeper,

contain smaller droplets, rain less frequently, and appear brighter from above in the presence of large concentrations of small aerosol particles. Ice-containing clouds, in the presence of small aerosol particles, generally contain smaller particles than cleaner clouds and exhibit weaker precipitation.

Direct aerosol radiative forcing depends on the optical depth of the aerosol layer and the ratio of the scattering to the sum of scattering and absorption (the single scattering albedo). The optical depth is related directly to the mass of aerosol, whereas the single scattering albedo depends on the relative composition of scattering and absorbing components. Overall global aerosol mass is strongly influenced by aerosol and precursor emissions inventories and atmospheric lifetime of particles. Emission inventories for particulate matter are not known to high accuracy. The predominant removal mechanism for atmospheric particles is wet deposition (precipitation), and climate models differ in their representation of wet removal. The combination of uncertain emissions and uncertain wet removal rates produces a substantial uncertainty of total airborne aerosol mass. Aerosol optical properties depend on the extent to which scatting and absorbing species are comixed in the same particles, and the extent of overall cooling vs. heating also depends on the vertical distribution of aerosols relative to clouds. The uncertainty concerning mixing state and vertical distribution is largely responsible for the wide range of estimates of forcing attributable to black carbon. Aerosol indirect forcing depends on the relationship between changes in aerosol levels and changes in cloud optical depth and lifetime. The cascade of processes that lead from aerosol, as characterized by size and composition, to cloud properties begins with activation of CCN to form cloud droplets. Once droplets are formed, whether precipitation results depends on the efficiency of autoconversion, the process by which precipitation-sized droplets are formed by droplet–droplet collisions. The parameterization of autoconversion in climate models is a source of uncertainty.[24] Nonetheless, as in the case of direct forcing, the uncertainty in aerosol abundance itself represents the dominant uncertainty in predicting aerosol indirect forcing.

Black carbon

Carbonaceous aerosol components, including black carbon and some forms of organic carbon, absorb strongly in the visible and ultraviolet wavelengths. Like all aerosols, black carbon (BC) scatters a portion of the incoming solar beam back to space, which leads to a reduction in solar radiation reaching the Earth's surface. A portion of the incoming solar beam is also absorbed by the black carbon. BC absorbs radiation yet again from the diffuse upward beam of scattered sunlight, reducing the solar radiation reflected back to space. (This effect is particularly accentuated when absorbing aerosols lie above clouds.) With a sufficiently absorbing aerosol, the surface cooling caused by radiation scattering back to space can be compensated for by the heating caused by absorbed radiation, leading to little net change in the radiative balance at the top of the atmosphere. This redistribution of energy has important potential feedbacks on atmospheric convection, precipitation, and the hydrological cycle. The rise of aerosols since preindustrial times has led to both a substantial reduction in solar radiation at the surface and increased solar heating of the atmosphere itself. Estimating the amount by which BC emissions have increased since preindustrial times is difficult owing to uncertain knowledge of the historical extent of biomass burning.

Black carbon results from incomplete combustion of carbonaceous matter (fossil fuels, biomass). Black carbon (also referred to as soot or elemental carbon) is seldom emitted alone from combustion; it is usually accompanied by organic carbon (OC). A mixture of BC/OC that is dominated by BC is a predominantly absorbing aerosol that leads to warming, whereas a low BC/OC ratio gives a predominantly scattering aerosol that leads to cooling. The BC/OC ratio for a particular combustion source depends on the fuel and the type of combustion. In emissions from fossil fuel burning the ratio of BC mass to OC mass is initially high (BC/OC > 1). In diesel emissions the aerosol is nearly pure BC. In emissions from open vegetation fires, BC/OC is initially low (<1). As aerosols age in the atmosphere, the BC/OC ratio of the particles will decrease due to condensation of gaseous organics, changing the radiative properties of the carbonaceous aerosol.

When BC particles become coated by nonabsorbing aerosol components via coagulation and condensation processes, the light absorption by these mixed particles becomes amplified. While a coating of BC with nonabsorbing material also increases the aerosol light scattering cross section, the overall single scattering albedo (the ratio of scattering to the sum of scattering and absorption) of the internally mixed particle is smaller than the externally mixed case, causing an increase in net atmospheric light absorption. Optical calculations based on realistic assumptions, as well as in situ observations, indicate that light absorption amplification owing to coating of BC lies in the range of 1.5 to 2. Knowledge of the extent to which BC particles are mixed with non-light-absorbing secondary compounds such as sulfate and nitrate is required for accurate radiative transfer calculations of the direct effect of anthropogenic aerosols. The mixing state of BC is generally assumed when calculating global aerosol climate forcing. Several representations of internally mixed BC sulfate particles have been used for optical calculations, predominantly a core-shell model and a particle uniformly mixed at the molecular level. The core-shell model seems most consistent with measurements of the optical properties of aged BC from coupled chemical-optical in situ aerosol time-of-flight mass spectrometer measurements.[25] Externally mixed BC leads to a calculated top of the atmosphere (TOA) forcing ranging from 0.2 to 0.4 W m^{-2}, while TOA forcing estimates for internally mixed, core-shell model, BC range from 0.4 to 1.2 W m^{-2}. This range of forcing lies between that calculated for CO_2 (1.66 W m^{-2}) and CH_4 (0.48 W m^{-2}), causing BC to be the second largest component contributing to planetary warming.

Coating of initially nonhygroscopic BC by soluble hygroscopic salts dramatically increases particle hygroscopicity, thus increasing the particle's ability to act as a CCN. The increased concentration of atmospheric CCN produced by coated BC particles also increases the rate of removal by wet scavenging and thus reduces its atmospheric burden and

lifetime. This increased rate of removal can counteract some or all of the amplified absorption of solar radiation by BC, particularly in remote regions.[26] The atmospheric lifetime, rate of hydrophobic to hydrophilic conversion, and mass burden of BC, as represented in global climate models, are an important source of uncertainty in the range of aerosol radiative forcings predicted by different models.

Two more effects involving BC need to be considered when calculating the radiative effect of BC particles:

- the semi-direct effect: the fact that absorbing particles in and around clouds heat up the atmosphere and lead to the evaporation of the cloud.[27]

- the ice-snow albedo effect: the deposition of absorbing particles on snow and ice reduces reflectivity and potentially leads to earlier melting.

These effects enhance the warming by BC, as they reduce the reflectivity of clouds and of a portion of the Earth's surface. Depending on the altitude of BC aerosol relative to clouds, the BC-induced heating can lead to either an increase or decrease of cloud cover. Isaksen et al.[28] report a range of -0.25 to $+ 0.50$ W m^{-2} for semidirect BC forcing.

Mitigation of BC has been suggested as a strategy complementary to reduction of greenhouse gases.[29,30] Any perturbation that affects the global aerosol number concentration has the potential to alter CCN concentrations and cloud properties. Depending on the fraction of BC primary particles that eventually become CCN, BC mitigation would affect global CCN concentrations, possibly leading to a change in global cloud radiative forcing from warm clouds. If such a perturbation were to result in a reduction in TOA cloud cooling, the amount of that reduction would oppose the amount by which the TOA direct BC heating is also reduced. To investigate this phenomenon, Chen et al.[31] considered two present-day mitigation scenarios: 50% reduction of primary black carbon/organic carbon (BC/OC) mass and number emissions from fossil fuel combustion (termed HF), and 50% reduction of primary BC/OC mass and number emissions from all primary carbonaceous sources (fossil fuel, domestic biofuel, and biomass burning) (termed HC). The Chen et al.[31] study is based on two key assumptions: (1) a decrease in BC mass emissions would be accompanied by a decrease in primary particulate number emissions, which would lead to a lower global aerosol number concentration and (2) by virtue of internal mixing with hydrophilic aerosol components, BC is assumed to contribute to the CCN population. Radiative forcing effects of these two scenarios were assessed through present-day equilibrium climate simulations. Global average top-of-the-atmosphere changes in radiative forcing for the two scenarios, relative to present day changes were calculated to be $+0.13 \pm 0.33$ W m^{-2} (HF) and $+0.31 \pm 0.33$ W m^{-2} (HC). Even less is known about the effects of BC, and indeed aerosols in general, on mixed phase or ice clouds; Isaksen et al.[28] suggest a range of forcing estimates -0.5 to $+0.5$ W m^{-2} with no best estimate.

Jones et al.[32] have identified the pattern of surface warming produced by BC in the observational record for the second half of the 20th Century, using climate simulations with a coupled atmosphere-ocean general circulation model. They divided the temperature responses into four categories, those due to: natural forcings, GHGs, factors other than BC (aerosols other than BC, ozone, land-use changes), and BC. While natural forcings did not contribute significantly to the temperature trends, the other three groups did. Notably, the warming effect of BC is discernable in the record. This finding is important because of the varied influences of BC on climate. As noted above, changes of BC levels can, in principle, affect global CCN concentrations. If increases in BC are reflected in increased CCN concentrations globally, then this could lead to an increase in cloudiness and a cooling effect. The analysis of Jones et al.[32] shows that the overall climatic effect of BC is one of warming. Despite any effect of BC mitigation on reduction of cloud cooling, which is at present highly uncertain, these results point to the beneficial effect of BC reduction on climate warming.

Lifetimes of climate forcing agents

Climate forcing agents, gases and aerosols, have a wide range of atmospheric lifetimes. Particles (aerosols) have an atmospheric lifetime of at most a few weeks. The response of global temperature to a change in CO_2 emissions will occur initially over the several-decade characteristic time of climate change but will continue to evolve slowly over the $>$1000 year lifetime of CO_2.[33] A corresponding change in aerosol emissions will result in a new atmospheric aerosol level within weeks. Still, the full climatic effect of that change will not be realized until the several-decade climate response time. The inherent climate change timescale also applies to the response to reductions in levels of climate forcing agents. Part of the accelerating trend in global warming during the last three decades can be attributed to the success of air pollution controls that have lead to a reduction mainly of sulfate and nitrate aerosols. Further reductions in levels of particulate matter required to protect human health will continue to contribute to global warming.[34]

Cosmic Rays and Climate

Galactic cosmic rays (GCRs) are the high-energy particles that flow into our solar system from far away in the Galaxy. GCRs are mostly pieces of atoms: protons, electrons, and atomic nuclei that have had all of the surrounding electrons stripped during their high-speed (atmost the speed of light) passage through the Galaxy. Cosmic rays provide one of the few direct samples of matter from outside the solar system. The magnetic fields of the Galaxy, the solar system, and the Earth have scrambled the flight paths of these particles so much that one can no longer point back to their sources in the Galaxy. About 90% of the cosmic ray nuclei are hydrogen (protons), and about 9% are helium (alpha particles). Cosmic rays are the main source of ions in the free atmosphere. For ions in the ambient atmosphere, the rate of production is $<$30 ion pairs cm^{-3} s^{-1}. A steady state concentration of ions is $\sim$ 2000 ions cm^{-3}, and the time scale for ion–ion recombination is $\sim$ 6 minutes. Variations in the solar wind modulate the cosmic ray flux; when sunspot number is at its minimum, the cosmic ray flux is at its maximum and vice versa.

It has been suggested that a connection exists between solar activity, through its effect on galactic cosmic rays, and

global warming of the past several decades.[35] The mechanism involves the effect of the cosmic ray flux on the generation of atmospheric ions, which serve as nucleation sites for formation of ultrafine particles,[36] some of which then grow large enough to become cloud condensation nuclei. The cosmic ray-climate hypothesis is: A decrease in solar activity leads to an increase in GCRs, leading to an increase in the rate of ion production in the atmosphere and in the ambient ion concentration. An increase in the ion concentration leads to an increase in particle formation by ion-induced nucleation. Increased levels of atmospheric aerosols lead to an increase in CCN concentrations, which produces enhanced cloud coverage and a cooler climate. Global warming could result from reduced cloud cover owing to variation of the solar-induced cosmic ray flux, or vice versa.

The galactic cosmic ray flux to the lower atmosphere varies by $\sim$ 15% over the 11-year solar cycle, with higher cosmic ray fluxes at the minimum of the cycle. Proxies for the cosmic ray flux indicate that the flux has decreased over the past century by an amount roughly equal to its variation over a solar cycle.[37] Because low clouds exert a strong cooling effect on climate, any mechanism that can affect global low clouds, by even a few percent, has the potential to exert significant leverage on climate. New particles form in the atmosphere by nucleation of vapor molecules, and it is well established that nucleation is enhanced by the presence of ions, so-called ion-induced nucleation. Freshly nucleated particles have diameters of about 1 nm. The CCN upon which low (stratus) clouds form need to be about 80–100 nm in diameter. Freshly nucleated particles grow in the atmosphere by condensation of vapor molecules, such as sulfuric acid and organics, and to function as CCN, they must grow into the 80–100 nm range. More numerous CCN lead to clouds with more numerous, but smaller, droplets; such clouds tend to have a higher albedo than their lower concentration counterparts, reflecting more sunlight back to space and cooling the Earth. As noted above, it has been hypothesized that a decrease in cosmic ray intensity, which leads to a decrease in atmospheric ion formation and thus in new particle formation, thereby leads to a decrease in CCN and a decrease in low cloud cover.

From a climate point of view, the atmospheric particle number concentration is most important in determining the CCN concentration, that is, those particles that can activate to form cloud droplets at water supersaturations prevailing in the atmosphere. The rate at which new particles form (nucleation) helps govern the overall number concentration of particles. Despite long recognition of this, the rates at which and the mechanisms by which nucleation occurs in the atmosphere are still the subject of intense interest.[38] This is a result of the sheer difficulty of duplicating atmospheric nucleation in the laboratory and the considerable challenge of sampling and measuring fresh sub-nm sized atmospheric nuclei. Add to this the role of ions, and the experimental and theoretical challenges are substantial. Sulfuric acid vapor is almost always the nucleating species; if certain organic molecules, like amines, are present, the rate of sulfuric acid nucleation is enhanced. And if ions are present as well, the nucleation rate is enhanced even further. Also, we know that there is virtually never sufficient sulfuric acid vapor present to condense on and grow a freshly nucleated particle to CCN size; organics are needed for this.

The critical quantity in the cosmic ray/cloud linkage is the fraction of nucleated particles that survive to reach CCN size, as sufficient vapor may not be available for their growth or many may be scavenged by coagulation with preexisting particles.[39] A significant fraction of CCN results from particles emitted directly by sources, such as combustion and sea salt, and nucleated particles that do survive to reach CCN size must "compete" with the myriad of these primary particles. Finally, most of the ionization potential of cosmic rays is at high altitude and high latitude; to affect low cloud formation at low latitudes, the CCN must be significantly transported.

Pierce and Adams[40] have carried out global aerosol simulations for years with high (solar min) and low (solar max) cosmic ray fluxes, approximately corresponding to years 1986 and 1990, respectively, leaving all other model parameters unchanged. The two cases considered were intended to capture the extent of change in mean cosmic ray flux over the past century. Throughout most of the free troposphere, the ion-pain production rate changes by 15–30% between the solar minimum and maximum, with changes less than 10% in the layer closet to the Earth's surface. The authors considered two ion nucleation rate models, the upper limit model assuming that every ion produced, positive or negative, will nucleate a particle provided that there is enough sulfuric acid vapor to condense on the particle and grow it to 1 nm. CCN concentrations at 0.2% water supersaturation (a typical supersaturation reached in low stratus clouds) are highest in the Northern Hemisphere mid-latitude lower troposphere and are dominated by direct emissions from anthropogenic sources. After accounting for all the intervening atmospheric physics, the sensitivity of CCN at 0.2% supersaturation to changes in the nucleation rate between the solar maximum and solar minimum was found to be very low.

The calculated insensitivity of CCN to changes in aerosol nucleation from varying cosmic ray flux is a consequence of the competitive physical processes involving small particles in the atmosphere. At faster nucleation rates, more nm-sized particles compete for the available condensable gases to grow to CCN sizes. Each particle grows more slowly and thus remains longer at the small sizes at which the particles are subject to efficient coagulation scavenging by other particles. Despite the fact that more particles have formed, the probability of any one particle surviving to reach CCN size is much lower. And, even if fewer CCN were generated by cosmic rays, it does not necessarily follow that global cloud formation would be inhibited, as in many regions of the Earth ample CCN exist from both natural and anthropogenic sources. All of these processes act to strongly dampen the sensitivity of CCN concentration to changes in the new particle formation rate.

For a demonstrable effect of galactic cosmic rays on climate, it would be necessary that the cosmic ray flux exhibit a clear and significant long-term downward trend. Such a trend, however, is not seen (Figure 5). Analyses of atmospheric data find no evidence of changes in cloud cover from changes in cosmic ray fluxes.[42–44]

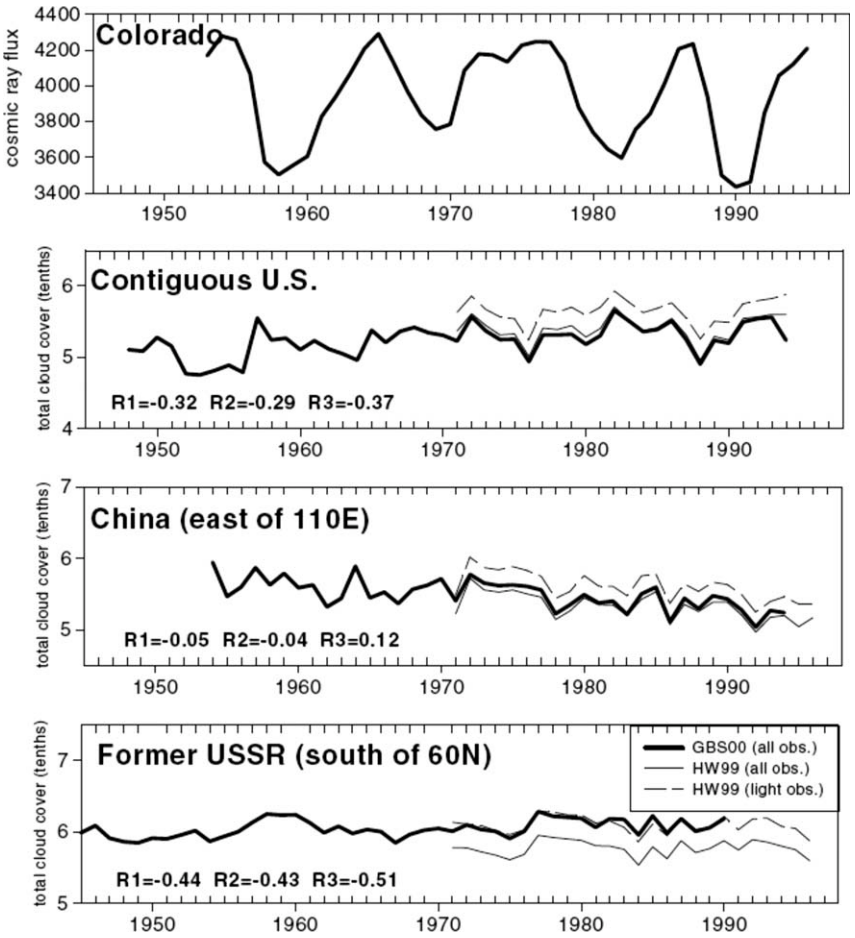

Figure 5. Galactic cosmic ray intensity from roughly 1950 to present day.[41]

Total Estimated Anthropogenic Forcing

Table 1 summarizes the IPCC[1] estimates and uncertainty bars (5–95% confidence range) on forcing from all important climate agents. Total forcing from the increase in CO_2 over the industrial period is + 1.66 W m^{-2}. Increase in CH_4, N_2O, chlorofluorocarbons, and tropospheric O_3, in aggregate, are estimated to produce a forcing of + 1.33 W m^{-2}, a value close to that of CO_2 itself. (The decrease in stratosphere O_3 due to chlorofluocarbons is estimated to produce a slight cooling effect.) Forcings resulting from changes in surface albedo are estimated to produce both warming and cooling effects, with a slight net cooling. Aerosols, on the whole, exert a cooling effect on climate, with direct forcing estimated as −0.5 W m^{-2}. The indirect climate forcing (effect of aerosols on cloud albedo) was estimated as −0.7 [−1.1, + 0.4] W m^{-2}, and no estimate was given of the forcing attributable to the effect of aerosols on cloud lifetime. Thus, the total aerosol forcing was estimated as −1.2 W m^{-2}. This can be compared with the total forcing due to GHGs and tropospheric O_3 of +3.0 W m^{-2}. Thus, according to the IPCC estimate, aerosols reduce GHG + O_3 forcing by 40%, globally.

Aerosol forcing is the most uncertain component of overall anthropogenic climate forcing, and the forcing attributable to black carbon represents a substantial part of that uncertainty. Anthropogenic BC direct forcing is estimated from climate model simulations[1] to range from 0.2 to 0.6 W m^{-2}. There is considerable uncertainty in estimated preindustrial BC forcing, ranging from 0.05 to 0.08 W m^{-2}[45] to 0.35 W m^{-2}.[46]

Myhre[47] addressed the consistency between satellite-derived and modeled estimates of the direct aerosol effect. BC aerosols and emissions have increased more than a factor of 6 since preindustrial time. Anthropogenic-influenced scattering aerosols have increased by a factor of ∼ 3 to 4. Myhre estimated the change in global aerosol single scattering albedo from preindustrial to present as 0.986 to 0.970. Because the absorbing fraction changed from 0.014 to 0.030, the particles are estimated to have become twice as absorbing in present times. Accounting for this change in the scattering/absorbing properties of the global aerosol does allow a closer reconciliation between satellite- and model-derived estimates of direct aerosol forcing. Myhre[47] arrived at a best estimate of current day direct aerosol forcing of −0.3 ± 0.2 W m^{-2}. Note the comparison with the IPCC best estimate of direct aerosol forcing of −0.5 W m^{-2}.

The forcing resulting from the increase in concentrations of long-lived GHGs and ozone from preindustrial time to

Table 1. Radiative Forcings Since Preindustrial Time[1]

Species	Radiative forcing (W m^{-2})
Long-lived greenhouse gases	
CO_2	$+1.66 \pm 0.17$
CH_4	$+0.48 \pm 0.05$
N_2O	$+0.16 \pm 0.02$
Halocarbons	$+0.34 \pm 0.03$
Total	$+2.63 \pm 0.26$
Ozone	
Stratospheric*	-0.05 ± 0.10
Tropospheric	$+0.35$ [-1.0, $+0.3$]
Stratospheric H_2O vapor from CH_4	$+0.07 \pm 0.05$
Aerosol	
Total direct	-0.50 ± 0.40
Indirect (cloud albedo)	-0.70 [-1.1, $+0.4$]
Solar irradiance	$+0.12$ [$-0.06 + 0.18$]

*A reduction in stratospheric O_3 affects surface temperature in two ways: (1) less stratospheric O_3 implies that more solar radiation will reach the surface-lower atmosphere system, which will tend to warm the climate; but (2) less stratospheric O_3 will lead to a cooler stratosphere (due to less absorption of solar radiation by O_3) that leads to less downwelling infrared radiation to the surface-lower atmosphere system, which will tend to cool the climate. The net effect on climate is smaller than either of the two effects taken alone, and the sign of the net effect depends on the altitudes where the O_3 change takes place. A reduction in O_3 at higher altitudes leads to net warming; a reduction of O_3 at lower altitudes leads to net cooling.

present day is ~ 2.9 W m^{-2} (Table 1). This quantity is 78% of the forcing corresponding to $2xCO_2$. If one takes the IPCC best estimate of ΔT_{2xCO_2} of 3°C, then the equilibrium increase in global mean temperature to present day is ~ 2.3°C. As this is an equilibrium value, one needs to add ~ 0.6°C of unrealized warming to the actual observed temperature rise of 0.8°C, to obtain a value of ~ 1.4°C, well below that based on the estimated climate sensitivity. As the expected ΔT that would result from $2xCO_2$ substantially exceeds the observed increase of 0.8 K for the entire 2.0–4.5 K range, for climate sensitivity to be the sole explanation for the temperature discrepancy, the actual climate sensitivity would have to be even lower than the IPCC lower limit, a result that IPCC termed "very unlikely." The IPCC best estimate of net global aerosol forcing from all climate agents combined is -1.2 W m^{-2} (5–95% range -0.6 to -2.4 W m^{-2}). The magnitude of aerosol forcing is substantial when compared with the GHG forcing of $+2.67$ W m^{-2}. (At this level aerosol cooling is offsetting 45% of GHG warming). Given the uncertainty associated with the aerosol forcing itself, the inescapable conclusion is that aerosol forcing is the most important uncertainty in determining climate sensitivity.

If the actual magnitude of aerosol forcing is close to the low end of its estimated uncertainty range, then the aerosol forcing offsets a considerably smaller fraction of the GHG forcing, and the total net global forcing is at the high end of its range, ~ 2.4 W m^{-2} (see also Schwartz[48]). At the other extreme, if the actual aerosol forcing is at the high end of its estimated range, then aerosol forcing is currently offsetting a major fraction of GHG forcing, and the total net global forcing is only ~ 0.6 W m^{-2}. For the observed global-mean temperature increase over the industrial period of 0.8°C, these two extremes of estimated global net forcing have major implications in terms of climate sensitivity:

$$\lambda \sim \frac{0.8^{\circ}\mathrm{C}}{2.4\ \mathrm{W\ m^{-2}}} = 0.33^{\circ}\mathrm{C\ W^{-1}\ m^{2}}$$
(low end of aerosol forcing)

$$\lambda \sim \frac{0.8^{\circ}\mathrm{C}}{0.6\ \mathrm{W\ m^{-2}}} = 1.33^{\circ}\mathrm{C\ W^{-1}\ m^{2}}$$
(high end of aerosol forcing)

The factor of four difference in climate sensitivity translates into the following range of estimates of equilibrium ΔT_{2xCO_2}

$$\Delta T_{2\times CO_2} \cong 1.2^{\circ}\mathrm{C} \qquad \text{(low end of aerosol forcing)}$$

$$\Delta T_{2\times CO_2} \cong 4.9^{\circ}\mathrm{C} \qquad \text{(high end of aerosol forcing)}$$

As the forcing from GHGs is well constrained, if present-day negative aerosol forcing is larger, the climate sensitivity consistent with the observed temperature change must itself be larger. This relationship is shown in Figure 6 in which ΔT_{2xCO_2} is a function of the assumed net aerosol forcing. If net aerosol forcing (negative) exceeds -1.2 W m^{-2}, then the amount of "cancellation" of GHG warming is even greater; consequently, the implied climate sensitivity to produce the actual observed temperature increase must be larger. At a present-day aerosol forcing of -2.0 W m^{-2}, for example, the climate sensitivity to $2xCO_2$ must be almost 4.5°C; at a net aerosol forcing of -1.0 W m^{-2}, the $2xCO_2$ sensitivity is close to 1.5°C. The shaded area in Figure 6 represents the climate sensitivity range of 1.5 to 4.5°C for $2xCO_2$. A range of aerosol forcings from about -0.5 to -2.0 W m^{-2}encompasses the range of climate sensitivities from 1.5 to 4.5°C. At the IPCC estimate of total aerosol forcing of -1.2 W m^{-2}, the GISS Model E, which was used to produce Figure 6, predicts a climate sensitivity of 2°C for $2xCO_2$. Schwartz et al.[49] provide a more complete

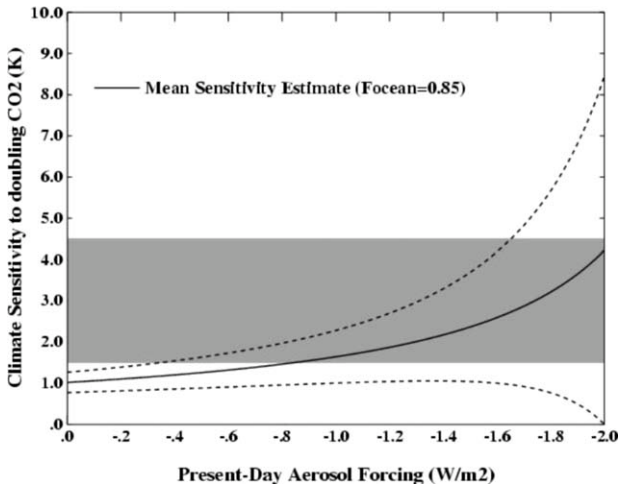

Figure 6. Climate sensitivity to doubling of CO_2 from its preindustrial level (°C) as a function of assumed present-day net aerosol forcing (W m^{-2}), as computed by Goddard Institute for Space Studies (GISS) Model E for the 20th Century (Gavin Schmidt, personal correspondence).

Excess ocean heat content = 0.85 W m^{-2}.

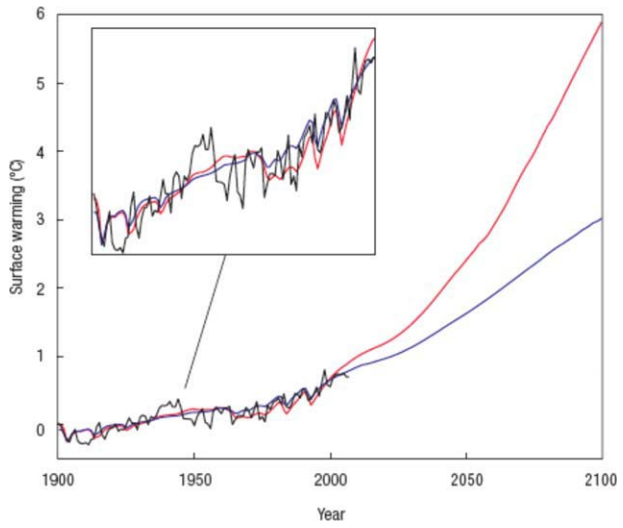

Figure 7. Simulation of observed warming over the 20th Century with a low climate sensitivity and high net forcing (2°C, 2.5 W m^{-2}; blue line) and a high climate sensitivity and low net forcing (6°C, 1.4 W m^{-2}; red line).

Figure reproduced from Knutti and Hegerl.[50] [Color figure can be viewed in the online issue, which is available at wileyonlinelibrary.com.]

discussion on the interplay between aerosol forcing and climate sensitivity.

The observed global warming up to present day can be simulated with different combinations of net radiative forcing and climate sensitivity. Knutti and Hegerl[50] illustrated this with a climate model of intermediate complexity used to simulate global temperature with a low climate sensitivity and a high total forcing over the 20th Century (2°C, 2.5 W m^{-2}) and with a high climate sensitivity and low net forcing (6°C, 1.4 W m^{-2}). Their results, shown in Figure 7, indicate that while both combinations can match observed 20th Century warming, that projected for the 21st Century based on standard emission scenarios will be quite different depending on the climate sensitivity.

In summary, uncertainty in global forcing attributable to aerosols translates into an uncertainty in climate sensitivity based on the observed change in global temperature over the last few decades. If the value of present-day aerosol (negative) forcing is deemed to be larger, the inferred climate sensitivity is also larger; in other words, if the cooling effect of aerosols is larger, the sensitivity of climate change (the amount of warming as a result of a change in forcing) must be larger to be consistent with the observed temperature rise. In the presence of sustained emissions of aerosols and their precursors, the overall cooling effect of aerosols will continue to offset a portion of the warming by GHGs. Owing to the roughly 2-week tropospheric residence time of aerosols, this continued replenishment of aerosol levels conflicts with attempts to reduce global air pollution. On the other hand, an abrupt decrease in aerosol levels would lead to a jump in temperature as a result in the increase in net positive forcing.[34,51,52]

Simplified Dynamic Description of Climate Forcing and Response

As only one-half of the Earth is illuminated at any time, the incoming solar energy flux is the product of the solar constant, S_o, the projected area of the sphere, πR^2, and (1-A), where A is the shortwave albedo of the Earth (the fraction of incoming radiation that is immediately reflected back to space). The outgoing longwave radiation flux is the product of the entire area of the planet, $4\pi R^2$, and the Stefan-Boltzmann flux, σT^4 (assuming, for the moment, a longwave emissivity ε of unity), where σ is the Stefan-Boltzmann constant (5.67×10^{-8} W m^{-2} K^{-4}). For the Earth, $A \cong 0.3$.[53] At equilibrium, the global average effective temperature of emission is

$$T = \left[\frac{S_o\,(1-A)}{4\sigma}\right]^{1/4} \tag{1}$$

With $S_o = 1370$ W m^{-2} and $A = 0.3$, Eq. 1 predicts $T = 255$ K. The actual global average surface temperature of the Earth's surface is $\sim$ 288 K. As the longwave radiation emitted by the Earth originates not just from the Earth's surface but also from the atmospheric itself, which is substantially colder than the surface, $T = 255$ K is a measure of the overall equilibrium temperature of the Earth-atmosphere system. The top-of-the-atmosphere radiative balance does not reveal the surface temperature or the vertical distribution of temperature in the atmosphere.

Response to a perturbation of the Earth's radiative equilibrium

Consider a perturbation in the Earth's energy balance such that the absorbed shortwave radiation and emitted longwave radiation are no longer in balance. Then, the Earth's temperature will change to re-establish equilibrium. Although a detailed evaluation of the transient response of Earth's energy balance requires a full-scale climate model, many key features of a transient climate response can be extracted from a single-compartment model of the atmosphere-land-ocean system. If H denotes the total heat content of the Earth system (in units of J m^{-2}) and F is the imposed forcing, then the energy balance is

$$\frac{dH}{dt} = F = \frac{1}{4}\,(1-A)\,S_o \;-\; \varepsilon\,\sigma\,T^4 \tag{2}$$

dH/dt can be expressed as

$$\frac{dH}{dt} = C\,\frac{dT}{dt} \tag{3}$$

where C (J m^{-2} K^{-1}) is an effective heat capacity of the Earth system that represents only that portion of the global heat capacity that is coupled to the perturbations on the time scale of the perturbation.[54] Then the transient temperature response is governed by

$$C\,\frac{dT}{dt} = \frac{1}{4}\,(1-A)\,S_o \;-\; \varepsilon\,\sigma\,T^4 \tag{4}$$

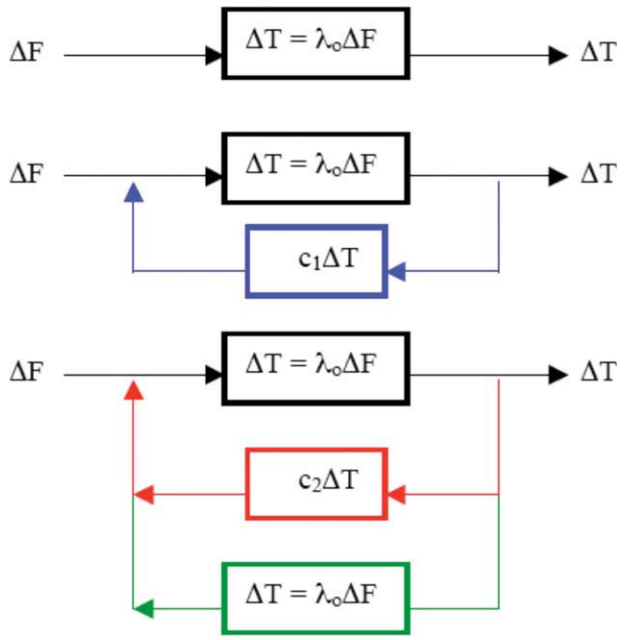

Figure 8. Block diagram representation of climate feedback processes.

[Color figure can be viewed in the online issue, which is available at wileyonlinelibrary.com.]

Suppose at the time of the perturbation, the Earth is at an equilibrium global temperature T_i. The transient temperature T can be expressed as $T_i + \Delta T$, where ΔT, the temperature change, will generally be small as compared to T_i. (For example, for $T_i \cong 255$ K, ΔT might be the order of a few K.) The new equilibrium corresponding to the sustained perturbation is given by

$$0 = \frac{1}{4}(1-A)\,S_o - \varepsilon\,\sigma\,(T_i + \Delta T_\infty)^4 \tag{5}$$

The fact that ΔT is small relative to T_i can be exploited in determining the transient response as governed by Eq. 4. Let us write (4) as

$$C\,\frac{d\Delta T}{dt} = F\,(T_i + \Delta T) \tag{6}$$

where $F(\cdot)$ is again just the imposed forcing. We can expand the R.H.S. of (6) in a Taylor series as

$$\begin{aligned} C\,\frac{d\Delta T}{dt} &= F\,(T_i) + \Delta T\,\frac{\partial F}{\partial T}\Big|_{T_i} \\ &= F\,(T_i) + 4\,\varepsilon\,\sigma\,T_i^3\,\Delta T \end{aligned} \tag{7}$$

Assuming that A and ε do not depend on T, the solution of (7) is

$$\Delta T\,(t) = \frac{F\,(T_i)/\,C}{4\,\varepsilon\,\sigma\,T_i^3\,/\,C}\left[1 - \exp\left(-\frac{4\,\varepsilon\,\sigma\,T_i^3\,t}{C}\right)\right] \tag{8}$$

The time constant for relaxation of the Earth's temperature to the new equilibrium temperature is

$$\tau = \lambda_o C \tag{9}$$

where $\lambda_o = (4\varepsilon\sigma T_i^3)^{-1}$ (K W^{-1} m^{-2}). As $t \to \infty$, the equilibrium temperature change is

$$\Delta T_\infty = \lambda_o F \tag{10}$$

where λ_o is the blackbody equilibrium climate sensitivity. For $T_i = 225$ K and an assumed infrared emissivity $\varepsilon = 1$, $\lambda_o = 0.27$ K W^{-1} m^{-2}. A more accurate value of λ_o derived from General Circulation Model calculations is $\lambda_o = 0.31$ K W^{-1} m^{-2}.[55] As noted earlier, the fact that the actual climate sensitivity λ is considerably larger than λ_o is the result of climate feedbacks.

Climate feedbacks

The energy balance expresses a relationship between the change in forcing, ΔF, and the change in temperature, ΔT. That a change in forcing leads to a blackbody change in temperature is depicted by the top panel of Figure 8, depicting the fundamental blackbody response ΔT_o from the temperature dependence of the infrared emission rate according to the Stefan-Boltzmann law, $\Delta T_o = \lambda_o\,\Delta F$, where λ_o is the parameter that accounts only for the Stefan-Boltzmann response. As global T increases, for example, the absolute concentration of atmospheric water vapor increases, leading to even more absorption of longwave radiation, and ice and snow are replaced by the more absorptive sea or land surfaces, leading to a decreased albedo A and even more absorption of solar radiation. In short, the climate system itself acts as an amplifier of externally imposed radiative forcing, via a positive feedback.

This feedback is depicted by the second panel in Figure 8, in which the initial blackbody change in temperature feeds back, with coefficient c_1, adding to the initial forcing ΔF. Then the full temperature response is

$$\Delta T = \lambda_o(\Delta F + c_1\,\Delta T) \tag{11}$$

and the resulting temperature change is

$$\Delta T = \frac{\lambda_o\,\Delta F}{1 - c_1\,\lambda_o} \tag{12}$$

The term $c_1\lambda_o$ can be termed the feedback factor. The ratio of the actual temperature change to the blackbody change can be called the gain, that is, the amount by which the temperature increases over the blackbody change due to the presence of the feedback,

$$G = \frac{\Delta T}{\Delta T_o} \tag{13}$$

and letting $f = c_1\lambda_o$, the gain is

$$G = \frac{1}{1-f} \tag{14}$$

With several feedbacks (see third panel of Figure 8),

$$\Delta T = \frac{\lambda_o \Delta F}{1 - \lambda_o \sum_i c_i} = \frac{\Delta T_o}{1 - \lambda_o \sum c_i} \tag{15}$$

With $f_i = c_i\ \lambda_o$, the gain is

$$G = \frac{1}{1 - \sum_i f_i} = \frac{1}{1 - f} \tag{16}$$

Although individual feedback factors are additive, the combined gain is greater due to the compounding effect of the positive feedbacks on each other.

Physical interpretation of feedback factors

Equation 4 can be expressed as

$$C\ \frac{dT}{dt} = F(T) \tag{17}$$

where $F(T)$ is the R.H.S. of (4), the radiative imbalance. Starting from a steady state $F(T_i) = 0$, and applying a sustained perturbation ΔF, the climate system will act to restore radiative equilibrium $F\ (T_i + \Delta T) = 0$. At any time, the change in the radiative imbalance can be written as

$$\delta F = \frac{\partial F}{\partial T}\ \delta T \tag{18}$$

Integrating between the onset of the perturbation and the new steady state yields

$$\int_{\Delta F}^{0} \delta F = \int_{T_i}^{T_i + \Delta T_\infty} \frac{\partial F}{\partial T}\ \delta T \tag{19}$$

Assuming linear behavior in the vicinity of the steady states, it follows that

$$\Delta F = -\left.\frac{\partial F}{\partial T}\right|_{T_i} \Delta T_\infty \tag{20}$$

From $\Delta T_\infty = \lambda\ \Delta F$,

$$\lambda^{-1} = -\left.\frac{\partial F}{\partial T}\right|_{T_i} \tag{21}$$

Differentiating (4) with respect to T yields

$$\lambda^{-1} = 4\sigma\varepsilon T_i^3 + \frac{S_o}{4}\left.\frac{\partial A}{\partial T}\right|_{T_i} + \sigma T_i^4 \left.\frac{\partial \varepsilon}{\partial T}\right|_{T_i} \tag{22}$$

The blackbody climate sensitivity λ_o, as in (10), is

$$\lambda_o^{-1} = 4\sigma\varepsilon T_i^3 \tag{23}$$

and λ can be expressed as in (15),

$$\lambda = \frac{\lambda_o}{1 - \lambda_o\ (c_1 + c_2)} \tag{24}$$

where

$$c_1 = -\frac{S_o}{4}\ \frac{\partial A}{\partial T}|_{T_i} \qquad c_2 = -\sigma\ T_i^4\ \frac{\partial \varepsilon}{\partial T}|_{T_i} \tag{25}$$

Feedback 1 is related to the change in planetary albedo with changing temperature, and feedback 2 describes the change in infrared emissivity with changing temperature. Planetary albedo changes include cloud and snow/ice feedbacks. Changes in emissivity with temperature include water vapor and atmospheric lapse rate feedback. The feedback factors f_i in (16) are identified as

$$f_1 = \lambda_o\ c_1 \qquad f_2 = \lambda_o\ c_2 \tag{26}$$

The range of variation of equilibrium temperature increases predicted for $2xCO_2$ is a result of the different ways in which climate models simulate processes internal to the climate system that either amplify or dampen the climate system's response to external forcing. Those climate feedbacks that directly affect the top-of-the-atmosphere radiation budget and do not involve chemical or biochemical processes in the biosphere or oceans involve water vapor, clouds, tropospheric temperature gradient (so-called temperature lapse rate), and surface albedo in snow/ice regions. The temperature lapse rate in the troposphere (i.e., the rate of decrease of temperature with altitude) affects the atmospheric transmission of infrared radiation to space; the steeper the decrease of temperature with height, the larger the greenhouse effect. Clouds strongly modulate the Earth's radiation budget, and the response of clouds to a global temperature change is a substantial part of the overall feedback effect. Of the global climate feedbacks, the water vapor feedback is the strongest.

Principal climate feedback parameters and gains, as deemed most probable by IPCC, are given in Table 2. The summation of c_i leads to a value of 1.91 W m^{-2} K^{-1}. With $\lambda_o = 0.31$ K W^{-1} m^2, it follows that $\lambda = 0.76$ K W^{-1} m^2. For discussions of climate feedbacks, we refer the reader to Bony,[56] Soden and Held,[55] Roe and Baker,[57] and Roe.[58] Water vapor feedback amplifies the global temperature response by a factor of 2 or more. Lapse rate feedback acts to dampen a warming response by about 20%. The mean value of predicted cloud feedback acts to amplify warming by about 30%, and surface albedo feedback leads to about 10% amplification of warming.

Climate Feedbacks

Water vapor feedback and lapse rate feedback

Water vapor is a natural constituent of the Earth's atmosphere, and it is the principal absorber of longwave infrared

Table 2. Climate Feedback Parameters and Gains[1]

	c_i (W m^{-2}/K)	$G_i = \frac{1}{1-\lambda_o c_i}$
Water vapor	1.80 ± 0.18	2.27
Lapse rate	–0.84 ± 0.26	0.80
Clouds	0.69 ± 0.38*	1.28
Surface albedo	0.26 ± 0.08	1.09

*Dessler[66] derived a value of 0.54 ± 0.74 (2σ). See text.

radiation emitted from the surface of the Earth. Even at the current level of atmosphere CO_2, water vapor makes up at least 50% of the greenhouse effect; CO_2 constitutes about 20%. The amount of water vapor in the atmosphere is determined by a balance between evaporation, principally from the oceans, and removal via precipitation. The mean atmospheric lifetime of a H_2O molecule is about 10 days; this means that, following any perturbation, a new water vapor equilibrium is established in a couple of weeks. (Too much water vapor in the air will rain out; too little, and more evaporates from the oceans, over this time scale). A positive feedback from water vapor is supported by basic physical theory and by many observations from ground- and space-based measurements.[59,60] Models have consistently predicted that, as warming takes place, atmospheric water vapor levels increase in a manner such that the relative humidity stays constant.[61] Detailed evaluations of data have shown that this prediction is essentially accurate. At the higher temperature, a constant relative humidity translates to a higher absolute concentration (specific humidity), so the total amount of water vapor in the air increases. Specifically, the water holding capacity of the atmosphere increases by 7% for each 1°C rise in temperature (as predicted by the Clausius-Clapeyron relation).

Once the H_2O concentration rises, the additional infrared absorption by the increased H_2O amplifies the initial warming through a powerful feedback effect. A test of the ability of climate models to simulate the water vapor feedback effect was afforded after the 1991 eruption of Mt. Pinatubo in the Philippines.[62] The volcanic aerosol caused global cooling for more than 2 years after the eruption. From the observed amount of sulfate aerosol emitted by the volcano, models were able to predict the observed decrease in water vapor resulting from the cooling induced by the aerosol.

Climate models predict that the concentration of H_2O vapor will increase in the upper troposphere as a result of increases in GHGs. Satellite measurements show a signature of upper tropospheric moistening over the period 1982–2004,[63] in accordance with predictions. This result was especially important in establishing the validity of treatment of water vapor feedback by climate models. Water vapor near the surface has little influence on the top-of-the-atmosphere balance, because the temperature of the air near the surface is close to that of the surface itself. By contrast, the relatively small quantity of water vapor aloft has a substantial influence on the top-of-the-atmosphere energy budget, because it increases the infrared opaqueness of these layers that are much colder than the surface. In so doing, this H_2O vapor blocks the upwelling infrared from the warmer parts of the atmosphere and replaces it with infrared emissions from the cold layer. Soden et al.[63] analyzed satellite data to compare mid- to upper tropospheric H_2O vapor observations with general circulation model predictions for the 1982−2004 period. The data indicate that upper-level moisture increases in warmer conditions, in the same manner as predicted by models. Moreover, by artificially suppressing moisture changes in synthetic data, they were able to definitively reject the hypothesis that upper troposphere water vapor content would remain constant as temperature increases.

The water vapor feedback process results mainly from changes in water vapor concentrations in the tropical upper troposphere.[59] In this region of the atmosphere, temperatures are well below those at the surface, and the water vapor lies above most of the clouds. Water vapor in this region is transported by the large-scale circulation, which conserves specific humidity (the ratio of the mass of water vapor to the total mass of a unit volume of air).[64] Thus, the water vapor feedback is essentially controlled by large-scale dynamics and the outflow of tropical deep convective systems. All global climate models predict a strong water vapor feedback. A spread among models in the magnitude of water vapor feedback is largely compensated by an opposite spread in the lapse rate feedback, which is a negative feedback that arises because a warmer atmosphere emits more infrared radiation to space, thereby reducing net surface warming. It turns out that the sum of the two feedbacks is about half the magnitude of the water vapor feedback and is quite consistent among climate models. Although both observations and models suggest that the magnitude of the water vapor feedback is similar to that if relative humidity remains constant in the atmosphere everywhere, this should not be construed to mean that RH is exactly constant everywhere; regional variations will occur, but they will have a negligible effect on the global feedback.

With respect to the water vapor and lapse rate feedback, at low latitudes climate models predict a larger warming at altitudes than near the surface, leading to a negative lapse rate feedback. At mid and high latitudes, by contrast, models predict a larger warming near the surface, i.e., a positive lapse rate feedback. On a global average, the tropical lapse rate response dominates, and the climate change lapse rate feedback is negative. Although all climate models predict this response, its magnitude varies among models. Intermodel differences in global lapse rate feedbacks are primarily a result of different meridional patterns of surface warming; the larger the ratio of tropical to global warming, the larger the negative lapse rate feedback. In summary, water vapor feedback is virtually certain to be strongly positive, with most evidence supporting a magnitude of 1.5 + 2.0 W m^{-2} K^{-1}. Thus, water vapor feedback alone roughly doubles the amount of warming that would otherwise occur.

Cloud feedback

Solar and terrestrial radiative properties of clouds have offsetting effects in terms of Earth's energy balance. In the infrared, clouds generally reduce the radiation emission to space and thus lead to a heating of the planet. In the solar region of the spectrum, clouds reflect sunlight back to space and thus produce a cooling. In areas covered by deep cumulus clouds, almost all of the incoming solar radiation is

reflected back to space. The cold cloud tops radiate very little energy to space. High, thin cirrus clouds, which often form from the outflow of moist air in the cumulus anvils, reflect some solar radiation back to space but also let some through to the Earth's surface. They emit some longwave energy both to space and back to the surface.

In the tropics, large-scale overturning circulations are associated with intense deep convective regions and widespread cloud-free regions of sinking motion. Nearly all of the upward motion occurs within deep cumulus clouds, with gentle subsidence between clouds. At midlatitudes, the atmosphere is organized in synoptic weather systems. The tropics and extratropics are characterized by a number of cloud types, from low-level boundary layer clouds to deep convective clouds. The distribution of cloud types is controlled by the large-scale atmospheric circulation as well as the surface boundary conditions, wind shear, etc. In the tropics, atmospheric dynamics control to a large extent changes in cloudiness. Boundary layer cloud amount is strongly related to the cloud types present, which depend on a number of factors. In the midlatitude regions clouds are controlled by the large-scale atmospheric dynamics.

The earth radiation budget experiment (ERBE), employing the NASA earth radiation budget satellite, launched in 1984,[65] has provided key data on the net radiative cloud effect. Results from ERBE indicate that, at present in the global mean, clouds reduce the radiative heating of the planet. The degree of cooling depends on season and ranges from about -13 to -21 W m^{-2}. On the basis of hemispheric averages, longwave and shortwave cloud forcings tend to balance each other in the winter hemisphere. In the summer hemisphere, the negative shortwave cloud forcing dominates the positive longwave cloud forcing, leading to a net cooling.

The net climatic effect of clouds is about –20 W m^{-2}. The cloud feedback contribution to climate feedbacks is a quantification of how this net effect changes as the Earth warms. If the result of a warmer climate is a further reduction in net incoming energy, the feedback would be negative; if a warmer climate leads to an increase in net incoming energy, then a positive feedback results. Virtually all climate models predict that cloud feedback is positive, i.e., changes in clouds in a warmer climate will further amplify warming, but the range of predicted values for the feedback factor is quite large, ranging from near zero to ~ 1 W m^{-2} K^{-1} (see Table 2). This spread is the largest contribution to the overall spread in climate sensitivities among climate models. Dessler[66] obtained an estimate of global cloud feedback in response to short-term climate fluctuations over the last decade, the main source of which is the El Niño—Southern Oscillation (ENSO). During the El Niño phase, monthly and global-average surface temperatures are several tenths of a degree Celsius warmer than during the La Niña phase. (These oscillations have been used to quantify the water vapor feedback.) Dessler[66] analyzed monthly and global-average anomalies of TOA net radiative flux between March 2000 and February 2010 measured by the Clouds and Earth's Radiant Energy System (CERES) instrument onboard the NASA Terra satellite. Over this time period, the cloud feedback had a magnitude of 0.54 ± 0.74 (2σ) W m^{-2} K^{-1}. No evidence to support a negative cloud feedback was found.

Summary of feedbacks

If we consider the principal feedbacks acting in concert, Eq. 16 predicts that $G = 2.45$, and for $2xCO_2$, $\Delta T_o = 1.2°C$ and thus $\Delta T \cong 3°C$. Roe and Baker[57] have shown the effect of uncertainty in the feedback factor f on the gain $G = \Delta T/\Delta T_o$ (Figure 9). The feedback factor f is assumed to be described by a probability density function h_f (f), the mean of which is at $f = 0.65$, with a standard deviation of 0.13, typical of that obtained in feedback studies with global climate models. Note that the mean value of f assumed by Roe and Baker[57] of 0.65 differs somewhat from the value of $f = 0.59$ inferred from the individual feedback factors in Table 2. The dot-dashed lines in Figure 9 represent 95% confidence intervals on the distribution of f and the resulting distribution of ΔT. The mean value of f of 0.65 implies a value of $\Delta T = 3°C$. Because the $G = 1/(1\text{-}f)$ relation is nonlinear, the distribution of ΔT is not symmetric. A value of f at its upper 95% confidence limit, exceeding 0.9 (highly unlikely), would translate into a ΔT of about 13°C. The lower 95% confidence limit on f, ~ 0.4, translates into $\Delta T \sim 2°C$. The individual climate feedback and the resulting overall feedback factor f differ among climate models owing to the particular representation of climate physics (essentially subgrid scale processes) in each model. As noted, cloud feedback is that with the most variability among climate models, which results from the intrinsic subgrid scale treatment of cloud processes in climate models.

Global Temperature Changes and the Paleoclimate Record

Temperature changes from preindustrial to present

The instrumental record of global temperatures has been the subject of considerable analysis as well as intense scrutiny. Figure 10 shows an analysis of the period 1880–2005 based on land data, satellite measurements of sea surface

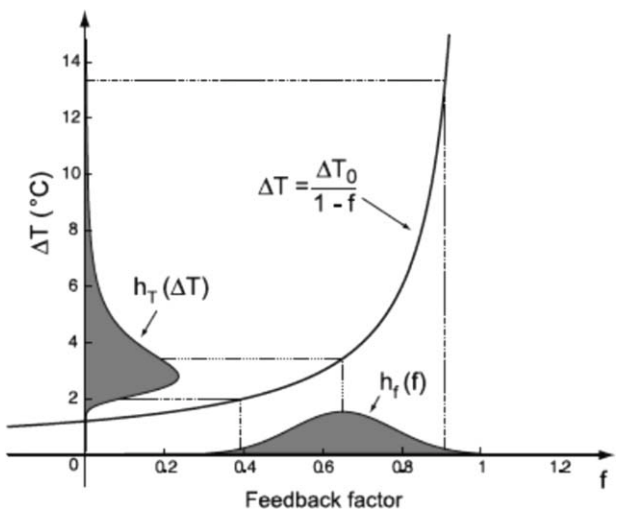

Figure 9. Relationship between the probability distribution of the feedback factor f, h_f (f) and that of ΔT_{2xCO_2}, $h_{\Delta T}$ (ΔT), as expressed by Eq. 16.[57]

temperature since 1982, and ship-based measurements in earlier years. Estimated 2σ (95% confidence) decreases from 0.1°C at the beginning of the 20th Century to 0.05°C in recent decades. The current warming is nearly worldwide, generally larger over land than over ocean, and largest at high latitudes in the Northern Hemisphere. Overall warming was about 0.7°C between the late 19th Century and year 2000. Slow warming, with large fluctuations, occurred over the century up to 1975, followed by rapid warming at a rate $\sim$ 0.2°C per decade. Thus, the total warming from the late 19th Century to year 2008 is about 0.8°C. The largest warming has taken place over remote regions, especially high latitudes. Warming occurs over ocean areas, far from direct human effects. Warming over the oceans is less than that over land; this is the expected response to a forced climate change because of the large thermal inertia of the ocean.

As the tropics warm, according to basic atmospheric physics, the upper atmosphere should heat up more than the surface. Comparison of data from radiosondes and satellites has generally confirmed this, although consistent long-term trends from both types of measurements are difficult to discern due to changes in calibrations, etc. Johnson and Xie[67] have used an independent method based only on observational records of sea surface temperature and precipitation to infer amplified warming in the upper troposphere, consistent with theory and climate models. Sobel[68] describes the physics underlying the relationship between sea surface and upper troposphere temperature. Consider an air parcel rising from close to the tropical ocean surface. Its temperature begins essentially as the sea surface temperature (SST), and its relative humidity is 80–90%. As the air parcel ascends and its temperature decreases, its water vapor condenses, producing the convective clouds that are prevalent in the tropics. As a result, the vertical atmospheric temperature profile (the so-called moist adiabat) becomes that of the rising air parcels. As the SST increases in response to global warming, both the temperature and absolute humidity of the surface air increase, so the rising air parcels follow a warmer moist adiabat than before. As these warmer and moister air parcels ascend, condensation of water vapor converts the additional latent energy in the water vapor into a less steep decrease of temperature. The new moist adiabat is warmer at all altitudes, but the amount by which it is warmer is larger at high altitudes owing to the fact that more and more of the water vapor will have condensed at the higher altitudes. The entire tropical atmosphere adjusts to the SST. The critical value of SST above which convection can occur is $\sim$ 27°C. Johnson and Xie[67] show that the SST threshold for convection has risen along with the tropical mean SST over the last few decades. This finding implies that the upper troposphere warms more than the surface. If the upper troposphere temperature had not increased more than that at the surface, then surface air parcels would not have to become as warm to rise and form rain. In that case, the SST threshold would be expected to remain roughly constant and not rise as observed. These results provide powerful independent confirmation of the expected response of the vertical structure of the atmosphere to global warming.

The three decades 1940–1970 were cooler than those preceding them. During this period sunspot activity and hence solar insolation was low. In addition, several volcanic eruptions occurred that led to enhanced stratospheric sulfate aerosol and its associated cooling. Also, emission controls on fine particles were generally absent or weak before 1970; as a result, tropospheric aerosol levels were high, leading to additional cooling. Based on satellite data from 1978 to 2002, the global troposphere (up to 10 km) has warmed at a rate of +0.22 to 0.26°C per decade, consistent with the warming trend derived from surface meteorological stations.[69] The Antarctic winter troposphere temperature has increased at a rate of 0.5 to 0.7°C per decade over the past 30 years.[70] The stratosphere has cooled since 1979, owing to ozone depletion.

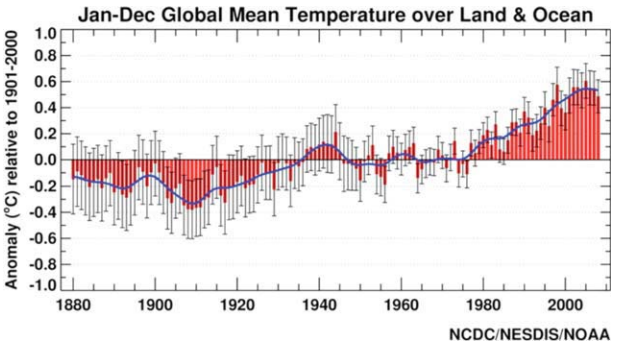

Figure 10. Global temperature anomaly (°C) as derived from surface air measurements at meteorological stations and ship and satellite measurements (NOAA and U.S. E.P.A.).

[Color figure can be viewed in the online issue, which is available at wileyonlinelibrary.com.]

In evaluating climate trends, one must distinguish between annual changes owing to internal oscillations (such as the tropical El Nino Southern Oscillation) and those due to external forcing. Outside of the tropics, the leading mode of variability in atmospheric circulation is an oscillation of atmospheric mass between mid- and high-latitudes in both the northern and southern hemispheres, that is, not due to the changing seasons, called annular modes. (The ENSO is a coupled ocean-atmosphere phenomenon, while the annular modes involve only atmospheric dynamics.) The annular modes appear as distinctive patterns in sea level pressure, temperature, and wind strength. Lower-than-normal pressure conditions (relatively less mass) over the poles is termed a high index or positive state. Climate models predict a shift toward a more uniformly positive state for the southern annular mode (SAM) under global warming, which is what has been observed over the last few decades. A shift to a more persistently positive SAM implies a poleward shift of the westerly jet stream, an intensification of westerly winds over the circumpolar ocean (at about 60° south latitude), and weaker westerlies farther north. The circumpolar ocean circulation intensifies as the SAM becomes more positive.

Aerosols diminish the amount of solar radiation reaching the Earth's surface, so-called "global dimming."[71,72] While GHGs are more or less evenly distributed over the entire globe, aerosols are disproportionately concentrated in the Northern Hemisphere. Based on this, one might expect proportionately more warming in the Southern Hemisphere, but

that is the opposite of what is observed. The explanation lies in the fact that uniform CO_2 concentrations do not imply uniform heating. Dynamical effects (changes in winds and ocean circulation) can exert as large an impact, locally, as GHG-induced forcing. Because the Northern Hemisphere contains disproportionately more land than the Southern Hemisphere, GHG-induced heating disproportionately affects the Northern Hemisphere. The ocean absorbs more heat without warming nearly as much, as it distributes heat rapidly in the upper layers via convection. Over land, most extra heat is transferred directly to the atmosphere. Another important factor is the difference in ocean dynamics between the Northern and Southern Hemisphere. Heat is mixed more efficiently into the deeper waters of the Southern Ocean. The interior of Antarctica has not warmed appreciably in the last few years. Thompson and Solomon[73] showed that the SAM has been in a more positive phase (stronger winds) in recent years; this acts as a barrier, preventing warmer mid-latitude air from reaching the continent, and may be a result of a combination of stratospheric O_3 depletion and stratospheric cooling owing to CO_2.[74]

Occurrence of extreme weather events

An issue that deserves mention is the relationship between the gradual trend of rising global temperatures and the occurrence of extreme weather events. Day-to-day weather varies; heat waves and extremes of cold weather occur every year. The probability distribution of temperature at a given location over a given period of time can be viewed as a bell-shaped curve. Extreme events at either end of the curve (very hot, very cold) will occur with a frequency roughly defined by the curve itself. A steady warming trend, which is what is meant by "climate change" or "global warming", shifts the entire curve to the right. As the right-hand tail of the curve moves to the right, the frequency of extreme warm events increases; likewise, at the other side of the curve, the frequency of extreme cold events goes down. There will still be extreme cold spells, but, averaged over a sufficiently long time, their frequency will decrease. No individual weather event can be said to have been "caused" by global warming. Heat waves have always occurred; it is difficult to prove that any individual heat wave today might not have happened even if all the greenhouse gases had not been emitted. But, on average, the pattern should be slowly changing: the frequency of record highs should be increasing, and that of record lows should be decreasing. This is exactly what the data show. The fact that it is bitter cold outside today says nothing about climate change. Similar comments pertain to precipitation extremes,[75] with respect to which recent work[76,77] indicates that warming that has occurred may already be influencing the intensity of rainfall.

The paleoclimate record

Records of past environmental changes are preserved in paleo archives, such as ice caps, marine and lake sediments, trees, and long-lived corals. Reconstruction of these records requires that the properties measured in natural archives (proxies) be quantitatively translated into environmental parameters. In so doing, the proxies must be rigorously calibrated against direct observations, such as air temperature or ocean salinity. Thus, a period of overlap between the proxy record and contemporary data is important for calibrating paleo-reconstructions. Most natural archives contain many lines of evidence; for example, a single ice core contains indications of air temperature, atmospheric gas composition, volcanic activity, and dust deposition rates. Proxy records must be dated so that the timing of events, rates of change, and relationships between different archives can be established. Chronologies are based on a variety of methods. Several of these, such as radiocarbon dating, depend on radioactive decay. Others rely on counting of annual layers, whether of snow accumulation, tree rings, seasonally deposited sediments, or volcanic ash layers. Accurately dated coral terraces provide estimates for sea level history for about the last 150,000 years.

Over the past 500,000 years, Earth's climate has varied cyclically between cold, glacial conditions and warm, interglacial periods. Warm, interglacial conditions have persisted for only short periods relative to the lengthy glacial ones. The cyclicity is driven by changes in the distribution of sunlight on the Earth's surface as the planet's orbit varies slightly through time. During glacial periods, the extent of ice on the land and surface ocean as well as variations in vegetation cover increase the reflectivity of the Earth's surface and reduce the amount of solar energy absorbed by the planet. Large parts of the Earth were drier, resulting in a dustier atmosphere, and more dust was deposited onto the ice sheets of Antarctica and Greenland and onto the surface of the ocean.[78] The glacial-age atmosphere was strikingly depleted of the greenhouse gases CO_2, CH_4, and N_2O.

Over the past 100,000 years, temperature changes in Greenland and the North Atlantic have paralleled each other. Notable features of this record are millennium-scale warm events, which are particularly marked in Greenland (increases of more than 10°C) but more subdued in the North Atlantic.[79] While not as clearly seen in the Greenland ice cores, several strong cooling events appear in the oceanic record, based on the presence in marine sediments of distinctive types of ice-rafted debris between 40 and 60 °N. The warm intervals are called Dansgaard-Oeschger (D/O) events in honor of Willie Dansgaard and Hans Oeschger who, in the early 1980s, identified and described the events in Greenland ice cores. The importance of the cold events was first recognized by Hartmut Heinrich in the late 1980s. The so-called Heinrich events originated mainly from melting of the Laurentide ice sheet covering Canada.

Even in regions of the Earth far from the North Atlantic, there is a clear atmospheric signature of D/O events. Atmospheric CH_4 concentrations peaked during every warm episode. As methane concentrations are globally uniform, they can be used to synchronize high-resolution ice core records from Greenland and Antarctica. Inferred temperatures in Antarctica show a slow warming that preceded the abrupt warming in the Northern Hemisphere by 1000–2000 years. As the north finally warmed (within less than a century), a slow cooling began in the Southern Hemisphere. This out-of-phase warming and cooling between Greenland and Antarctica reflects changes in the surface and deep water circulation of the Atlantic and associated exchanges of heat.[80]

As noted earlier, a business-as-usual trajectory of fossil-fuel energy generation will lead to a CO_2 level of $\sim$ 900 to 1100 ppm by 2100. Reconstructions of atmospheric CO_2

concentrations indicate that it has been $\sim$ 30 to 100 million years as such a level existed in the atmosphere.[81] Paleoclimate data also reveal that it took tens of millions of years for the CO_2 level to decline to those of the more recent past. When CO_2 was $\sim$ 1000 ppm at $\sim$ 35 million years ago, tropical to subtropical sea surface temperatures were in the range of 35 to 40°C (vs. present day values of $\sim$ 30°C) and polar SSTs in the Southern Hemisphere were 20–25°C (vs. present day temperatures of $\sim$ 5°C).[82] At this time the Sun was less luminous by $\sim$ 0.4%. It is estimated that the net radiative forcing during this period $\sim$ 35 million years ago was $\sim$ 8 W m^{-2}. Global annual mean temperature at that time can be estimated as $\sim$ 31°C, vs. 15°C during preindustrial times.[83] The climate sensitivity inferred from the estimates of forcing and global mean temperature at that time is $\lambda \cong 16°C/8\ W\ m^{-2} = 2°C\ W^{-1}\ m^2$, at least a factor of two larger than current estimates. This discrepancy may be due to long time-scale feedback processes in land ice, vegetation, and the carbon cycle itself that do not enter into current climate model simulations.

Glacial-interglacial cycles

Periodic changes in the Earth's orbit around the Sun and in the tilt (obliquity) of the Earth's axis control the seasonal and latitudinal distribution of incoming solar radiation.[84,85] The time of year when the Earth is closest to the Sun varies with quasi-periodicities of about 19,000 and 23,000 years. The obliquity of the Earth's axis varies between 22 and 24.5° with a quasi-periodicity of about 41,000 years. When the tilt is greater, the poles are exposed to more sunlight.

Milutin Milankovic in the 1930s argued that glaciation occurs when solar insolation intensity is weak at high northern latitudes in summer. This occurs when both Earth's spin axis is less tilted with respect to the orbital plane and the aphelion (the point of Earth's orbit that is farthest from the Sun) coincides with summer in the Northern Hemisphere. When there is less insolation during summer, snow and ice persist through the year, gradually accumulating into an ice sheet. The trigger for an ice age depends on the intensity of Northern Hemisphere summer sun (i.e., whether the solar intensity is large enough to melt the ice that accumulates over winter). If the solar flux $<$475 W m^{-2} at 65 °N, then this is insufficient to melt the ice.

Over the last 900,000 years (740,000 of which are recorded in the oldest Antarctic ice core yet recovered), the full glaciation and deglaciation cycles exhibit a very distinctive, asymmetric pattern. Each cycle lasts about 100,000 years, with the bulk of that time ($\sim$ 90,000 years) devoted to slow cooling and the gradual growth of ice sheets toward a ''glacial maximum'' condition. The great changes in ice volume take place mainly in the Northern Hemisphere, though the Antarctic ice sheets grow as well. In contrast, deglacation is rapid, requiring 10,000 or fewer of those 100,000 years. Deglaciation is followed by relatively short (10–20,000 years, as recorded in a variety of climate proxies) warm interglacial intervals. Changes in Earth's orbit around the Sun is the one external climate forcing that operates on these time scales and is the cause of the glacial-interglacial cycles. However, changes in Earth's orbit alone cannot produce this very asymmetric cycle.

The large amplitude glacation and deglaciation cycles are the result of climate feedbacks in the global response to the external orbital forcing.[86] Ice sheets, sea ice, atmospheric circulation, atmospheric chemistry, the terrestrial and marine carbon cycles, and ocean circulation are all involved. Our understanding of how these components interact and produce the asymmetric, 100,000 year cycle comes from many lines of evidence.[87,88] At the onset of an ice age, the small initial cooling resulting from the orbital changes is then amplified as the CO_2 concentration falls. (At higher levels of CO_2, this trigger threshold decreases because the temperature is higher, i.e., an ice age is less likely.) The onset of the last ice age, about 116,000 years ago, corresponded to a 65 °N mid-June insolation about 40 W m^{-2} lower than today. There is general agreement that the CO_2 decrease at the onset of an ice age is related to changes in the carbon uptake by the oceans, with some theories relying on enhancement of the biological pump, but the actual mechanism has yet to be firmly identified. At the termination of a glacial maximum (defined by orbital forcing), atmosphere and ocean warming begins around Antarctica; this warming causes CO_2 to begin to return to the atmosphere from the deep ocean. The additional CO_2 produces additional warming, now of the whole planet, because CO_2 mixes quickly through the atmosphere.[89] The additional warming leads to even more CO_2 release to the atmosphere, etc. Estimates of the time lag for CO_2 feedback range from less than 200 years to about 800 years. The rapid transfer of carbon from the lithosphere to the atmosphere over the last century or so associated with the burning of fossil fuels is an unprecedented forcing in the climate system, driving change on a time scale of decades, not millenia.

A number of hypotheses exist to explain the low CO_2 concentrations during glacial times. The ocean is the most important of the relatively fast-exchanging ($<$1000 year) carbon reservoirs. On these timescales, atmospheric CO_2 is controlled by the interplay between ocean circulation, marine biological activity, ocean-sediment interactions, seawater carbonate chemistry, and air-sea exchange. CO_2 is more soluble in colder waters; so, changes in ocean temperature can alter atmospheric CO_2. The Southern Ocean is especially important in this regard because it is where large volumes of deep water masses are formed and where large amounts of biological nutrients upwell to the surface. Western Equatorial Pacific sea surface temperature was about 3°C colder during the last ice age than today. As this area of the ocean was relatively unaffected by changes in higher latitude ice cover and in ocean circulation, the cooling can be explained only in terms of changes in atmospheric GHGs. Support for the role for the Southern Ocean in controlling atmospheric CO_2 during glacial times is provided by the concurrent decrease of Antarctic temperature and atmospheric CO_2.

In summary, during a deglaciation, slow changes in orbital parameters cause greater amounts of summer sunlight to fall in the Northern Hemisphere. This relatively small change causes ice to retreat in the north, which decreases the albedo. The loss of reflecting surface leads to further warming in a feedback effect. About 600 years or so after that process starts, CO_2 and CH_4 concentrations began to rise, which amplifies the warming trend even more, and GHG forcing eventually takes over as the dominant factor in the ultimate

change. The 600-year time lag is consistent with the time required for CO_2 stored in the deep ocean to be brought up to the surface where it can be released to the atmosphere. CO_2 is also released from warming soils and CH_4 from melting permafrost. The end of the deglaciation is characterized by a clear CO_2 maximum. Evidence that temperature changes precede changes in CO_2 concentrations in some climate changes on the timescales of ice ages shows only that temperature changes can affect the atmospheric CO_2 concentrations, which in turn feed back on temperature changes. Such evidence has no bearing on the fact that the increase in greenhouse gas concentrations over the past century is human induced.

An empirical estimate of the Earth's climate sensitivity can be obtained from the change of conditions from the Last Glacial Maximum to the present, for which IPCC[1] estimated a change in forcing of –8 W m^{-2} and a range of change in global mean surface temperature of –4 to –7°C. The climate sensitivity range determined from these values is 0.5 to 0.875°C W^{-1} m^2, in general agreement with the range estimated by climate models based on changes from preindustrial conditions to the present.

The Holocene

The Holocene, now almost 12,000 years in duration, during which human civilization has developed, has been characterized by a remarkably stable climate, in which the planet is sufficiently warm for the great ice sheets of the Northern Hemisphere to be absent, but not warm enough for a disintegration of the Antarctica or Greenland ice sheets.

The only notable climate transition event during the Holocene occurred about 8200 years ago and was less intense and of shorter duration than the glacial swings. During the glacial period, the 4-km-thick Laurentide ice sheet significantly depressed the underlying land. During the long relaxation time scale (a few millennia) of Earth's viscoelastic rebound, the ice melted back into its own depression. Because the ice centered on Hudson Bay blocked off the outlet of the Bay, extensive lakes (including the largest lake on Earth at that time) formed around the ice and could not drain. Eventually, as the ice shrank, the meltwater escaped, likely emptying the largest lake on Earth into the North Atlantic over a time as short as a single summer to a few years. This event was immediately followed by a widespread cooling,[90] probably because the fresh water favored sea-ice formation in the North Atlantic.

A period of generally warmer temperatures due to increased solar activity was recorded mainly in western Europe between 1000 and 1200 and has been referred to as the Medieval Warm Period (MWP).[91,92] Although the extent of warming in the MWP is uncertain, analysis of a variety of proxy records indicates that the geographic extent of warming in the late 20th Century and early 21st Century substantially exceeds that during the MWP.[93] With enhanced solar irradiance, changes in large-scale circulation patterns associated with the Arctic Oscillation may explain why Europe was warmer in this period. During the MWP, the Northern Hemisphere average temperature reached that of the 1940s, but below current temperatures. The Little Ice Age (LIA) was an interval between $\sim$ 1400 and 1900 when temperatures in the Northern Hemisphere were generally colder than today's, especially in Europe. The LIA essentially consisted of two episodes (16th and 19th Centuries) with warming in between.

During the 10,000 years since the end of the last ice age, there were regional climate changes of substantial amplitude, and rapid short-term changes (e.g., in response to volcanic eruptions), but no similarly rapid and strong global warming as in the past decades. The Little Ice Age and Medieval Warm Period were not global or hemispheric in scale, but essentially local phenomena largely confined to Europe. The warming that has taken place in the 20th and 21st Centuries is larger, more rapid, and more globally extensive than any excursions over the past 2000 years. For a review of studies on climate over the last 1000 years or so, we refer the reader to Keller.[2]

Uncertainties in temperature reconstruction

Considerable attention has been paid to the reconstruction of temperature variations over time. Thermometer measurements over the past 150 years provide an unequivocal record of increasing temperatures, especially over the last several decades. Some have claimed that measured increases in temperature reflect the growth of cities and not global warming. Great care has been exercised to account for the effect of urbanization in temperature records by comparing data from stations near urban areas with those at rural locations. Most importantly, the largest temperature anomalies on Earth occur in remote areas like the Arctic and the Antarctic Peninsula. Temperature records before the advent of thermometer measurements rely on paleoclimate data from tree rings, coral reefs, lake sediments, stalagmites, glacial movements, and historical accounts. The thickness of tree rings, for example, reflects temperature and rainfall amounts. The statistics used to analyze tree ring data have come under question, especially those from a few northern sites, where tree growth tracked atmospheric temperatures for much of the 20th Century but began to diverge from actual temperatures over recent decades. It is suspected that tree growth may respond differently when temperatures exceed a certain threshold. The tree ring divergence problem is restricted to a few high-latitude regions of the Northern Hemisphere and is not ubiquitous even in these regions. Nonetheless, a better understanding of how different species of trees respond to climate change is needed to better interpret tree ring data.

Ice

Ice sheet mass balance

The yearly mass balance of an ice sheet or glacier accounts for the amount of new ice (the water equivalent contained in the snow) that accumulates and the amount of ice lost to melting or to the calving of icebergs. Given a glacier or ice sheet that is in equilibrium with a given climate state, if the climate cools, the area of the glacier subject to melting will likely decrease, but the amount of snow the glacier receives over the course of the year may also decrease. In a warming climate, more melting and more precipitation are both possible, and the extent to which the glacier recedes depends on the relative magnitudes of the additional melting

and any extra snow accumulation. With continued warming, the elevation of the transition from net mass gain to net mass loss (called the equilibrium line) moves higher, and eventually enhanced melting will outpace enhanced accumulation. Mass balance may be assessed in several ways: an accounting between annual net accumulation and annual discharge through outlet glaciers; satellite observation of change in surface height; or satellite observation of change in ice sheet mass (via gravitational attraction).[94]

The Greenland ice sheet

Greenland has been ice covered for about 3.3 million years, at which time a transition occurred from a mostly ice-free island to the ice-covered Greenland of today. There have been several competing theories as to why Greenland became ice covered; these include changes in ocean circulation, the increasing height of the Rocky Mountains, changes in Earth's orbit, and changes in atmospheric GHG concentrations. Lunt et al.[95] tested each of these theories using state-of-the-art climate and ice-sheet models. While the results suggest that climate shifts associated with changes in ocean circulation and tectonic uplift did affect the amount of ice cover, and that the ice waxed and waned with changes in Earth's orbit, none of these changes could explain the long-term growth of the Greenland ice sheet. The results suggest that the dominant cause of Greenland glaciation was the fall of atmospheric CO_2 from the relatively high level at that time to one closer to that of preindustrial times. Today, CO_2 concentrations are approaching the levels that existed when Greenland was mostly ice-free.

At 2.17 x 10^6 km^2 area, Greenland is slightly more than one-fifth the size of the continental U.S. It is, at present, about 80% ice covered. Greenland ice is equivalent to about 6 to 7 m of global sea level. In Greenland, both enhanced accumulation at high elevations and enhanced melting at low elevations are occurring. In Greenland, ice in the interior of the ice sheet flows slowly, 10's of meters per year (the ice is thick but relatively cold and surface slopes are small).[96] Ice moves away from the interior toward outlet glaciers that discharge ice into the sea. In 2005, Greenland's fastest outlet glaciers, Kangerdlugssuaq in the east and Jakobshavn in the west, were moving at about 12 kilometers per year at their downstream ends. Total snowfall has been increasing over Greenland. In the high, cold interior of the ice sheet the net effect is mass accumulation, while at lower elevations melting dominates. Melt season (typically April to September) duration has increased by up to a month since the late 1980's. The 2000 m elevation contour has served traditionally as a nominal boundary between the accumulation zone (above) and the ablation zone (below), although surface melting has been observed at higher and higher altitudes over time. As a result of enhanced surface melting and increases in outlet glacier flow, the Greenland Ice Sheet is losing a total volume of somewhere between 124 and 224 km^3 of ice per year.

Antarctica

Antarctica can be divided into three major geographic regions. The Transantarctic Mountains divide the continent into eastern (on the Indian Ocean side) and western (on the Pacific Ocean side) regions. The East Antarctic is a dry, vast snow-covered plateau atop a kilometers-thick ice sheet. The West Antarctic ice sheet stores enough ice to raise sea level between 5 and 6 m, and the East Antarctic Ice Sheet holds about 10 times more. (The total ice volume is larger than this but once the ice is melted, water fills the depression left behind.) The third region, the Antarctic Peninsula (AP), is a relatively mild temperature, narrow, mountainous chain extending north toward the Drake Passage. The AP plateau has a series of ice caps, which drain into mountain glaciers that eventually deliver the ice back to the sea. About 0.5 m of sea level equivalent ice is stored on the AP.

Sea ice

When sea ice begins to form at the ocean surface, it insulates the underlying water from additional cooling. Any new, first-year ice that persists through the summer and into fall and thickens again the following winter is classified as multiyear ice. Multiyear ice makes up a large proportion of the Arctic ice pack. This year-to-year persistence allows the old ice to grow quite thick, up to 4 or 5 m (thicknesses around the Antarctic are 1 to 2 m). The seasonal cycle of new ice production and melting in the Arctic basin yields a maximum ice extent in March and a minimum extent in September. As the atmosphere warms and the summer melt season intensifies, sea ice retreats, and the bright reflective surface is replaced with the dark ocean. The ocean surface absorbs more incoming solar radiation, and the warmer ocean surface radiates that energy back to the air above, amplifying the initial warming effect. This process delays the return to ice growth in the autumn, leading to a relatively thinner ice pack the following spring.

Remote sensing has established trends in sea ice extent. The era of high quality satellite observations began in late 1978 with the launch of NASA's Scanning Multichannel Microwave Radiometer, followed by the first Special Sensor Microwave/Imager in 1987. There has been a statistically significant downward trend in Arctic sea ice cover from 1979 to 2006, in every month of the year. The decline has been more rapid for September, the end of the melt season, for which the trend is $-8.6\% \pm 2.9\%$ per decade.[97]

Sea level change

There are two predominant sources of sea level change: thermal expansion or contraction of ocean water and net mass change from glaciers and ice sheets. Changes in the volume of water stored in aquifers and surface reservoirs can play a modest role in sea level change as well. The upper few 100 m's of the global ocean are warming, and the resulting thermal expansion is estimated to account for between 1/4 and 1/3 of the total observed sea level rise over the past century. Glaciers and ice sheets hold 75% of Earth's fresh water, the equivalent of about 75 m of sea level. About 90% is stored in the Antarctic ice sheets. Most of the rest, equivalent to about 7 m of global sea level, is stored in the Greenland Ice Sheet. Mountain glaciers hold an equivalent of $\sim$ 0.65 m of sea level.

Conclusion

The attribution of observed climate change is generally based on simulation of the climate of the last 150 years or so using climate models including all known and quantifiable forcings. Some of the forcings are well established (e.g., well-mixed GHGs, volcanic emissions, solar irradiance), while others are less certain (tropospheric aerosol effects, land use changes). Given the uncertainties, best estimates are made consistent with observations of the actual forcing agents. Certain observational facts serve to constrain the simulations. As the surface temperature and ocean heat content are rising together, intrinsic variability of the climate system can be ruled out as the cause of the recent warming. (Internal climate changes, such as ENSO or thermohaline variability, involve transfer of heat within the climate system, and therefore would occur only if energy is transferred to the atmosphere from another reservoir (i.e., the ocean), which itself would need to be cooling.) Our understanding of forcings and long-term observations of land surface and ocean temperature changes are consistent within the range of uncertainties.

Uncertainty in representation of physical processes at the spatial scale of climate models is the main source of differences in predicted climate sensitivity among models. The IPCC presents a list 54 ''key uncertainties'' which have received considerable scrutiny in the scientific literature; yet, none of these uncertainties challenges the scientific consensus of human-induced climate change. In a sensitivity study designed to explore the range of variation of models, Murphy et al.[98] varied 29 parameters, one by one, and analyzed the results of 20-year simulations under present day and $2xCO_2$ conditions. They computed probability density functions of climate sensitivity; in the 5–95% probability range, warming ($2xCO_2$) was determined to lie between 2.4 and 5.4°C. Even with the relatively wide range of systematic parameter variation, the fundamental responses of the climate models lie within the range derived from paleoclimate data.

The global temperature increase over the past century and a half can be simulated with various combinations of net radiative forcing and climate sensitivity (e.g., Figure 7). Although the observed temperature increase serves as a constraint that must be met by any simulation, the degree of freedom afforded by the net radiative forcing and the climate sensitivity acting in concert does not allow one to determine either with certainty. Cloud radiative feedback represents the leading source of uncertainty in the feedbacks that combine to determine climate sensitivity. The two largest components of the Earth's energy imbalance are the changes in GHGs (heating), which are known precisely, and the changes due to atmospheric aerosols (cooling), the overall measurement of which is not yet possible. As a result, the uncertainty in overall net radiative forcing is essentially attributable to aerosols. Remote sensing, in situ, and surface measurements are helping to close the uncertainties in aerosol forcing, but reducing the uncertainties attributable to aerosol forcing will require continued dedicated research that considers global emissions, microphysical processes, and in situ and remote sensing measurements. A ''top-down'' estimate of overall aerosol forcing was carried out by Murphy et al.,[99] who used measurements of ocean heat content, GHGs, volcanic aerosols, and correlations between surface temperature and satellite radiative flux measurements to infer a residual planetary energy flux that is presumed to be a result of aerosol direct and indirect radiative forcing. They inferred a total aerosol forcing of -1.1 ± 0.4 W m^{-2} for the period 1970–2000. This estimate cannot distinguish what aerosols are causing the forcing, how much of the forcing is due to indirect effects on clouds, or how the aerosol forcing is changing. While the existence of human-induced global warming is unequivocal, answers to the question, ''how much and how soon?'' bear upon these uncertainties.

Finally, most emissions scenarios for the next 50 to 100 years involve a substantial increase in GHG forcing. Given that most estimates of aerosol changes over the next century will not be proportionately as large as that of GHGs (and even for some substances, decreasing), future forcing can be expected to be increasingly dominated by GHGs, and aerosol cooling may assume an increasingly less important role as a mitigating factor in global warming.

Literature Cited

1. Intergovernmental Panel on Climate Change. *Climate Change 2007: The Physical Science Basis*. Cambridge, UK: Cambridge University Press, 2007.
2. Keller CF. Global warming: a review of this mostly settled issue. *Stochastic Environ Res Risk Assess*. 2009;23:643–676.
3. Trenberth KE, Fasullo JT, Kiehl J. Earth's global energy budget. *Bull Am Meteorol Soc*. 2009;90:311–323.
4. Nakicenovic N, Grubler A, McDonald A. *Global Energy Perspectives*. Cambridge, UK: Cambridge University Press, 1998.
5. Pollack H, Hurter S, Johnson J. Heat flow from the Earth's interior: analysis of the global data set. *Rev Geophys*. 1993;31:267–280.
6. Pierrehumbert RT. Infrared radiation and planetary temperature. *Physics Today*. 2011;64:33–38.
7. National Research Council. *Radiative Forcing of Climate Change*. Washington, DC: The National Academies Press, 2005.
8. Lacis AA, Schmidt GA, Rind D, Rudy RA. Atmospheric CO2: principal control knob governing Earth's temperature. *Science*. 2010:330;356–359.
9. Fröhlich C. Observations of irradiance variability. *Space Sci Rev*. 2000;94:15–24.
10. Bard E, Raisbeck GM, Yiou F, Jouzel J. Solar irradiance during the last 1200 years based on cosmogenic nuclides. *Tellus* 2000;52B:985–992.
11. Meehl GA, Washington WM, Wigley TM L, Arblaster JM, Dai A. Solar and greenhouse gas forcing and climate response in the twentieth century. *J Climate*. 2003;6:426–444.
12. Lean J, Rind D. Earth's response to a variable sun. *Science*. 2001;292:234–236.
13. Eichler A, Olivier S, Henderson K, Laube A, Beer J, Papina T, Gäggeler HW, Schwikowski M. Temperature response in the Altai region lags solar forcing. *Geophys Res Lett*. 2009;36:L01808. DOI: 10.1029/2008GL035930.
14. Shindell DT, Schmidt GA, Mann ME, Rind D, Waple A. Solar forcing of regional climate change during the Maunder minimum. *Science*. 2001;294:2149–2152.
15. Krivova NA, Solanki SK. Solar variability and global warming: a statistical comparison since 1850. *Adv Space Res*. 2004;34:361–364.
16. Camp CD, Tung KK. Surface warming by the solar cycle as revealed by the composite mean difference projection. *Geophys Res Lett*. 2007;34:L14703. DOI: 10.1029/2007GL030207.
17. Haigh JD, Winning AR, Toumi R, Harder JW. An influence of solar spectral variations on radiative forcings of climate. *Nature*. 2010;467:696–699.
18. Tedesco K, Feeley RA, Sabine CL, Cosca CE. Impacts of anthropogenic CO_2 on ocean chemistry and biology. *NOAA*. 2005. Available at www.oar.noaa.gov/spotlite/spot_gcc.html.

19. Gerlach T. Volcanic versus anthropogenic carbon dioxide. *EOS*. 2011;92:201–202.
20. Shindell DT, Faluvegi G, Bell N, Schmidt GA. An emissions-based view of climate forcing by methane and tropospheric ozone. *Geophys Res Lett*. 2005;32:L04803. DOI: 10.1029/2004GL021900.
21. Gauss M, Myhre G, Isaksen ISA, Grewe V, Pitari G, Wild O, Collins WJ, Dentener FJ, Ellingsen K, Gohar LK, Hauglustine DA, Iachetti D, Lamarque JF, Mancini E, Mickley LJ, Prather MJ, Pyle JA, Sanderson MG, Shine KP, Stevenson DS, Sudo K, Szopa S, Zeng G. Radiative forcing since preindustrial times due to ozone changes in the troposphere and lower stratosphere. *Atmos Chem Phys*. 2006;6:575–599.
22. Koren I, Kaufman YJ, Remer LA, Martins JV. Measurement of the effect of Amazon smoke on inhibition of cloud formation. *Science*. 2004;303:1342–1345.
23. Koren I, Martins JV, Remer LA, Afargan H. Smoke invigoration versus inhibition of clouds over the Amazon. *Science*. 2008;321: 946–949.
24. Penner JE, Quaas J, Storelvmo T, Takemura T, Boucher O, Guo H, Kirkevag A, Kristjansson JE, Seland O. Model intercomparison of indirect aerosol effects. *Atmos Chem Phys*. 2006;6:3391–3405.
25. Moffet RC, Prather KA. In-situ measurements of the mixing state and optical properties of soot with implications for radiative forcing estimates. *Proc Natl Acad Sci USA* 2009;106:11872–11877.
26. Stier P, Seinfeld JH, Kinne S. Boucher O. Aerosol absorption and radiative forcing. *Atmos Chem Phys*. 2007;7:5237–5261.
27. Hansen J, Sato, M, Ruedy R. Radiative forcing and climate response. *J Geophys Res*. 1997;102:6831–6864.
28. Isaksen ISA, Grainer C, Myhre G, Berntsen TK, Dalsoren SB, Gauss M, Klimont Z, Benestad R, Bousquet P, Collins W, Cox T, Eyring V, Dowler D, Fuzzi S, Jöckel P, Laj P, Lohmann U, Maione M, Monks P, Prevot ASH, Raes F, Richter A, Rognerud B, Schulz M, Shindell D, Stevenson DS, Storelvmo T, Wang WC, van Weele M, Wild M, Wuebbles D. Atmospheric composition change: climate-chemistry interactions. *Atmos Environ*. 2009;43:5138–5192.
29. Jacobson, MZ. Control of fossil-fuel particulate black carbon and organic matter, possibly the most effective method of slowing global warming. *J Geophys Res*. 2002;107:4410. DOI: 10.1029/ 2001JD001376.
30. Bond TC. Can warming particles enter global climate discussions? *Environ Res Lett*. 2007;2:045030.
31. Chen WT, Lee, YH, Adams PH, Nenes A, Seinfeld JH. Will black carbon mitigation dampen aerosol indirect forcing? *Geophys Res Lett*. 2010;37:L09801. DOI: 10.1029/2010GL042886.
32. Jones GS, Christidis N, Stott PA. Detecting the influence of fossil fuel and bio-fuel black carbon aerosols on near surface temperature changes. *Atmos Chem Phys*. 2011;11:799–816.
33. Archer D, Eby, M, Brovkin V, Ridgewell A, Cao L, Mikolajewicz U, Caldeira K, Matsumoto K., Munhoven G, Montenegro A, Tokos K. Atmospheric lifetime of fossil fuel carbon dioxide. *Annu Rev Earth Planet Sci*. 2009;37:117–134.
34. Raes F, Seinfeld JH. New directions: climate change and air pollution abatement: a bumpy road. *Atmos Environ*. 2009;43:5132–5133.
35. Friis-Christensen E, Lassen K. Length of the solar cycle: an indicator of solar activity closely associated with climate. *Science*. 1991;254:687–700.
36. Svensmark H. Influence of cosmic rays on Earth's climate. *Phys Rev Lett*. 1998;81:5027–5030.
37. Carslaw KS, Harrison RG, Kirkby J. Cosmic rays, clouds, and climate. *Science*. 2002;298:1732–1737.
38. Kirkby J, Curtius J, Almeida J, Dunne E, Duplissy J, Ehrhart S, Franchin A, Gagné S, Ickes L, Kürten A, Kupe A, Metzger A, Riccobono F, Rondo L, Schobesberger S, Tsagkogeorgas G, Wimmer D, Amorim A, Bianchi F, Breitenlechner M, David A, Dommen J, Downard A, Ehn M, Flagan RC, Haider S, Hansel A, Hauser D, Jud W, Junninen H, Kreiss F, Kvashin A, Laaksonen A, Lehtipalo K, Lima J, Lovejoy ER, Makhmutov V, Mathot S, Mikkilä J, Minginette P, Mogo S, Nieminen T, Onnela A, Pereira P, Petäjä T, Schnitzhofer R, Seinfeld JH, Sipilä M, Stozhkov Y, Stratmann F, Tomé A, Vanhanen J, Viisanen Y, Vrtala A, Wagner PE, Walther H, Weingartner E, Wex H, Winkler PM, Carslaw KS, Worsnop DR, Baltensperger U, Kulmala M. Role of sulphuric acid, ammonia and galactic cosmic rays in atmospheric aerosol nucleation. *Nature*. 2011;476:429–433.
39. Pierce JR, Adams PJ. Efficiency of cloud condensation nuclei formation from ultrafine particles. *Atmos Chem Phys*. 2007;7:1367–1379.
40. Pierce JR, Adams PJ. Can cosmic rays affect cloud condensation nuclei by altering new particle formation rates? *Geophys Res Lett*. 2009;36:L09820. DOI: 10.1029/2006GL037946.
41. Sun B, Bradley RS. Solar influences on cosmic rays and cloud formation. *J Geophys Res*. 2002;107:D14. DOI: 10.1029/2001JD000560.
42. Sloan T, Wolfendale AW. Testing the proposed causal link between cosmic rays and cloud cover. *Environ Res Lett*. 2008;3. DOI: 10.1088/1748-9326-3-2-0234001:1–6.
43. Calgovic J, Albert C, Arnold F, Beer J, Desorgher L, Fluedkiger EO. Sudden cosmic ray decreases: No change of global cloud cover. *Geophys Res Lett*. 2010;37:L03802. DOI:10.1029/2009GL041327.
44. Kulmala M, Riipinen I, Nieminen T, Hulkkonen M, Sogacheva L, Manninen E, Paasonen P, Petäjä T, Dal Maso M, Aalto PP, Viljanen A, Usoskin I, Vainio R, Mirme S, Mirme A, Minikin A, Petzold A, Hõrrak U, Plaß-Dülmer C, Birmili W, Kerminen V-M. Atmospheric data over a solar cycle: no connection between galactic cosmic rays and new particle formation. *Atmos Chem Phys*. 2011;10:1885–1898.
45. Bauer SE, Menon S, Koch D, Bond TC, Tsigaridis K. A global modeling study on carbonaceous aerosol microphysical characteristics and radiative effects. *Atmos Chem Phys*. 2010;10:7439–7456.
46. Hansen J, Nazarenko L, Ruedy R, Sato M, Willis J, Del Genio A, Koch D, Lacis A, Lo K, Menon S, Novakov T, Perlwitz J, Russell G, Schmidt GA, Tausnev N. Earth's energy imbalance: confirmation and implications. *Science*. 2005;308:1431–1435.
47. Myhre G. Consistency between satellite-derived and modeled estimates of the direct aerosol effect. *Science*. 2009;325:187–190.
48. Schwartz SE. Uncertainty in climate sensitivity: causes, consequences, challenges. *Energy Environ Sci*. 2008;1:430–453.
49. Schwartz SE, Charlson RJ, Kahn RA, Ogren JA, Rodhe H. Why hasn't Earth warmed as much as expected? *J Climate*. 2010;23: 2453–2464.
50. Knutti R, Hegerl GC. The equilibrium sensitivity of the Earth's temperature to radiation changes. *Nat Geosci*. 2008;1:735–743.
51. Brasseur GP, Roeckner E. Impact of improved air quality on the future evolution of climate. *Geophys Res Lett*. 2005;32:L23704. DOI: 10.1029/2005GL023902.
52. Matthews HD, Caldiera K. Transient climate-carbon simulations of planetary geoengineering. *Proc Natl Acad Sci USA* 2007;104:9949–9954.
53. Bender FAM, Rohde H, Charlson RJ, Ekman AML, Loeb N. 22 views of the global albedo-comparison between 20 GCMs and two satellites. *Tellus*. 2006;58A:320–330.
54. Schwartz SE. Heat capacity, time constant, and sensitivity of Earth's climate system. *J Geophys Res*. 2007;112:D24S05. DOI: 10.1029/ 2007JD008746.
55. Soden BJ, Held IM. An assessment of climate feedbacks in coupled ocean-atmosphere models. *J Climate*. 2006;19:3354–3360.
56. Bony S, Colman R, Kattsov VM, Allan RP, Bretherton CS, Dufresne JL, Hall A, Hallegatte S, Holland MM, Ingram W, Randall DA, Soden BJ, Tselioudis G, Webb MJ. How well do we understand and evaluate climate change feedback processes? *J Climate*. 2006;19: 3445–3482.
57. Roe GH, Baker MB. Why is climate sensitivity so unpredictable? *Science*. 2007;318:629–632.
58. Roe G. Feedbacks, timescales, and seeing red. *Annu Rev Earth Planet Sci*. 2009;37:93–115.
59. Held IM, Soden BJ. Water vapor feedback and global warming. *Annu Rev Energy Environ*. 2000;25:441–475.
60. Schneider T, O'Gorman PA, Levine XJ. Water vapor and the dynamics of climate changes. *Rev Geophysics*. 2010;48RG3001. DOI: 10.1029/2009RG000302:1–22.
61. Pierrehumbert RT, Brogniez H, Roca R. *On the relative humidity of the atmosphere*. In: Schneider T, Sobel AH, editors. *The Global Circulation of the Atmosphere*. Princeton, NJ: Princeton University Press; 2007.
62. Soden BJ, Wetherald RT, Stenchikov GL, Robock A. Global cooling after the eruption of Mount Pinatubo: a test of climate feedback by water vapor. *Science*. 2002;296:727–730.
63. Soden BJ, Jackson DL, Ramaswamy V, Schwarzkopf MD.Huang X. The radiative signature of upper tropospheric moistening. *Science*. 2005;310:841–844.

64. Dessler AE, Sherwood SC. A matter of humidity. *Science*. 2009;323:1020–1021.
65. Barkstrom BR. Earth radiation budget experiment (ERBE) archival and April 1985 results. *Bull Am Meteorol Soc*. 1989;70:1254–1262.
66. Dessler AE. A determination of the cloud feedback from climate variations over the past decade. *Science*. 2010;330:1523–1527.
67. Johnson NC, Xie SP. Changes in the sea surface temperature threshold for tropical convection. *Nat Geosci*. 2010;3:842–845.
68. Sobel A. Climate science: raised bar for rain. *Nat Geosci*. 2010;3:821–822.
69. Vinnikov KY, Grody NC. Global warming trend of mean tropospheric temperature observed by satellites. *Science*. 2003;302:269–272.
70. Turner J, Lachlan-Cope TA, Colwell S, Marshall GJ, Connolley WM. Significant warming of the Antarctic winter troposphere. *Science*. 2006;311:1914–1917.
71. Wild M, Ohmura A, Makowski K. Impact of global dimming and brightening on global warming. *Geophys Res Lett*. 2007;34:L04702. DOI:10.1029/2006GL028031.
72. Wild M. Global dimming and brightening: a review. *J Geophys Res*. 2009;114:D00D16. DOI: 10.1029/2008JD011470.
73. Thompson DWJ, Solomon S. Interpretation of recent southern hemisphere climate change. *Science*. 2002;296:895–899.
74. Shindell DT, Schmidt GA. Southern hemisphere climate response to ozone changes and greenhouse gas increases. *Geophys Res Lett*. 2004;31:L18209. DOI: 10.1029/2004GL020724.
75. Allan RP, Soden BJ. Atmospheric warming and the amplification of precipitation extremes. *Science*. 2008;321:1481–1484.
76. Min SK, Zhang X, Zwiers,FW, Hegerl GC. Human contribution to more-intense precipitation extremes. *Nature*. 2011;470:378–381.
77. Pall P, Aina T, Stone DA, Stott PA, Nozawa T, Hilberts AGJ, Lohmann D, Allen MR. Anthropogenic greenhouse gas contribution to flood risk in England and Wales in autumn 2000. *Nature*. 2011;470:382–385.
78. Lambert F, Delmonte B, Petit JR, Bigler M, Kaufmann PR, Hutterli MA, Stocker TF, Ruth U, Steffensen JP, Maggi V. Dust-climate couplings over the past 800,000 years from the EPICA Dome C ice core. *Nature*. 2008;452:616–619.
79. Bard E. Climate shock: abrupt changes over millennial trime scales. *Phys Today*. 2002;55:32–38.
80. Thornalley DJR, Barker S, Broecker WS, Elderfield H, McCave IN. The deglacial evolution of North Atlantic deep convection. *Science*. 2011;331:202–205.
81. Pagani M, Zachos JC, Freeman KH, Tipple B, Bohaty S. Marked decline in atmospheric carbon dioxide concentrations during the palaeogene. *Science*. 2005;309:600–603.
82. Bijl PK, Schouten S, Sluijs A, Reichart GJ, Zachos JC, Brinkhuis H. Early paleogene temperature evolution of the southwest Pacific Ocean. *Nature*. 2009;461:776–779.
83. Kiehl J. Lessons from Earth's past. *Science*. 2011;331:158–159.
84. Hays JD, Imbrie J, Shackleton NJ. Variations in the Earth's orbit: pacemaker of the ice ages. *Science*. 1976;194:1112–1131.
85. Berger AL. Long term variations of daily insolation and quaternary climate changes. *J Atmos Sci*. 1978;35:2362–2367.
86. Lorius C, Jouzel J, Raymond D, Hansen J, LeTreu, H. The ice-core record: climate sensitivity and future greenhouse warming. *Nature*. 1990;347:139–145.
87. Petit JR, Jouzel J, Raynaud D, Barkov NI, Barnola JM, Basile I, Bender M, Chappellaz J, Davis M, Delaygue G, Delmotte M, Kotlyakov VM, Legrand M, Lipenkov VY, Lorius C, Pépin L, Ritz C, Saltzman E, Stievenard E. Climate and atmospheric history of the past 420,000 years from the Vostok ice core, Antarctica. *Nature*. 1999;399:429–436.
88. Fischer H, Wahlen M, Smith J, Mastroianni D, Deck B. Ice core records of atmospheric CO_2 around the last three glacial terminations. *Science*. 1999;283:1712–1714.
89. Monnin E, Indermühle A, Dällenbach A, Flückiger J, Stauffer B, Stocker TF, Raynaud D, Barnola JM. Atmospheric CO_2 concentrations over the last glacial termination. *Science*. 2001;291:112–114.
90. von Grafenstein U, Erlenkeuser H, Müller J, Jouzel J.Johnsen S. The cold event 8200 years ago documented in oxygen isotope records of precipitation in Europe and Greenland. *Climate Dyn*. 1998;14:73–81.
91. Bradley RS, Hughes MK, Diaz HF. Climate in medieval time. *Science*. 2003;302:404–405.
92. Hughes MK, Diaz HF. Was there a 'Medieval Warm Period', and, if so, where and when? *Climatic Change*. 1994;26:109–142.
93. Osborn TJ, Briffa KR. The spatial extent of 20th-century warmth in the context of the past 1200 years. *Science*. 2006;311:841–844.
94. Luthcke SB, Zwally HJ, Abdalati W, Rowlands DD, Ray RD, Nerem RS, Lemoine FG, McCarthy JJ, Chinn DS. Recent Greenland ice mass loss by drainage system from satellite gravity observations. *Science*. 2006;314:1286–1289.
95. Lunt DJ, Foster GL, Haywood AM, Stone EJ. Late pliocene Greenland glaciation controlled by a decline in atmospheric CO_2 levels. *Nature*. 2008;454:1102–1111.
96. Rignot E, Kanagaratnam P. Changes in the velocity structure of the Greenland ice sheet. *Science*. 2006;311:986–990.
97. Stroeve J, Holland MM, Meier W, Scambos T, Serreze M. Arctic sea ice decline: faster than forecast. *Geophys Res Lett*. 2007;34:L09501. DOI: 10.1029/2007GL029703.
98. Murphy JM, Sexton DMH, Barnett DN, Jones GS, Webb MJ, Collins M, Stainforth DA. Quantification of modeling uncertainties in a large ensemble of climate change simulations. *Nature*. 2004;430:768–772.
99. Murphy DM, Solomon S, Portmann, RW, Rosenlof KH, Forster PM, Wong T. An observationally based energy balance for the Earth since 1950. *J Geophys Res*. 2009;114:D17107. DOI: 10.1029/2009JD012105.

Manuscript received Jul. 5, 2011, and revision received Sept. 12, 2011.